The effects of propofol on afterhyperpolarizations and synaptic transmission in CA1 pyramidal cells

Master's thesis in Molecular Biosciences

Daniel Kolnier

Master's thesis at The Department of Biosciences

UNIVERSITETET I OSLO

June, 2019

2019

The effects of propofol on afterhyperpolarizations and synaptic transmission in CA1 pyramidal cells

Daniel Kolnier

http://www.duo.uio.no/

Trykk: Reprosentralen, Universitetet i Oslo

Acknowledgements

The work presented in this thesis was performed at the Institute for Basic Medical Sciences, University in Oslo, under the supervision of professor Johan Frederik Storm and Nicholas Hagger-Vaughan.

First of all, I want to thank my supervisors. Johan for giving the opportunity to work in his lab, sharing his knowledge and experience with me, and for always being positive and approachable. Further, I want to thank Nick for his guidance, and for his patience throughout all the questions and broken equipment. Thank you both for showing me how fascinating neuroscience can be. I would also like to thank associate professor Marianne Fyhn, for the help and support you've given throughout my master.

I would also like to thank the rest of the Brain Signalling group, for helping me when I've needed it and for contributing to a good social environment. Special thanks to Yvette and Sarah for always helping each other out and sharing our frustrations.

Lastly, I would like to thank Mari, my friends, and my family for the support and encouragement.

Oslo, June 2019

Daniel Kolnier

Abstract

Consciousness is an important aspect of our life, and we spend the most part of our day in a conscious state. Little is known about the mechanisms of consciousness, and how the switch from a conscious state, such as wakefulness, to an unconscious state like sleep. During both slow wave sleep and general anesthesia, two different states of unconsciousness, a synchronization of neocortical activity can be observed, together with the emergence of an oscillatory pattern of depolarizations and hyperpolarizations in the membrane potential of cortical neurons. *In silico* models have shown the importance of the outward K^+ channel underlying the slow afterhyperpolarization (sAHP) in regulating the transition from a depolarized state to a hyperpolarized state, and for synchronization of neuronal activity during slow wave sleep.

I wanted to investigate whether propofol, a general anesthetic, could regulate the cellular oscillations observed in cortical neurons during slow wave sleep by increasing the slow afterhyperpolarization size. To do this, I performed whole-cell current clamp recordings in rat hippocampal slices on CA1 pyramidal cells. Application of propofol (5 μM) seemed to decrease the sAHP size in 1-hour long recordings. Due to unstable baseline recordings, this observed decrease could not with certainty be attributed to an effect of propofol. A significant decrease in the medium afterhyperpolarization (mAHP) amplitude was also observed. To determine the molecular target of propofol, I investigated the activity of two voltage-gated channels which are important for mAHP in CA1 pyramidal cells; the hyperpolarization-activated cyclic-nucleotide-gated channel (HCN channel) and the M-channel. I found no indication of change in HCN channel activity. In response to subthreshold depolarizations, the cells exhibited less inhibition after application of propofol, corresponding with a reduced M-channels conductance. A change in the spiking pattern after application of propofol was observed, similar to the changes observed in previous studies by inhibition of M-channels. Further, I investigated the effects of on synaptic transmission and found an increased excitatory postsynaptic potential (EPSP) amplitude after application of propofol, similar to those acquired from SK channel inhibition in previous reports. An increased $GABA_A$-mediated inhibtion was also found, corresponding to previous findings.
I conclude that propofol decreases mAHP amplitude, probably by M-channel inhibition, and also increases EPSPs, possibly by inhibition SK channels in CA1 pyramidal cells. Further studies are required to validate these findings.

List of abbreviations

Table 1.1: List of abbreviations

ACh	Acetylcholine	I_{sAHP}	sAHP current
aCSF	Artificial cerebrospinal fluid	ISIs	Interspike intervals
AHP	Afterhyperpolarization	LTP	Long-term potentiation
AMPAR	α-amino-3-hydroxy-5-methylisoxazole-4-propionic acid receptor	mAHP	Medium afterhyperpolarization
AP	Action potential	NMDAR	N-methyl-D-aspartate receptor
CA	Cornu Ammonis	non-REM	Non-rapid eye movement
CNS	Central nervous system	REM	Rapid eye movement
CSF	Cerebrospinal fluid	RMP	Resting membrane potential
EEG	Electroencephalogram	sAHP	Slow afterhyperpolarization
EPSP	Excitatory postsynaptic potential	SEM	Standard error of the mean
fAHP	Fast afterhyperpolarization	SK channel	Small conductance Ca^{2+}-dependent K^+ channels
$GABA_A$	γ-aminobutyric acid	SLM	Stratum lacunosum-moleculare
HCN channel	Hyperpolarization-activated cyclic-nucleotide-gated channel	SWA	Slow-wave activity
IK channel	Intermediate Ca2+-dependent K+ channel	SWS	Slow-wave sleep
I_{mAHP}	mAHP current		

Table of content

1 Introduction

1.1 Networks and brain states

1.1.1 Information encoding in the brain

Information in the brain is encoded through the activation of neurons leading to the generation of action potentials (APs). Both the frequency of activation and the timing of activation are important, but it is unlikely that a single neuron is solely responsible for conveying a message or for a physiological function. Our brains are constituted out of networks, where different types of neurons have their own role. In addition to the encodings of single cells, the information is contained in the *number* of cells active, *when* they are active, and the *types* of cells active.

Information is encoded on many levels, from the molecular and cellular, to how different brain areas communicate and how the two hemispheres co-operate. To understand how information is processed and how complex functions like emotions, personality traits, and consciousness arise from simple binary signals, all levels have to be explored.

1.1.2 Network activity and oscillations

When neurons and networks of neurons are activated, their membrane potential changes, leading to small extracellular currents and tiny changes in the electric field. Several different techniques, like electroencephalogram (EEG) and electrocorticography, are designed to measure these potentials. Many studies try to decode the information found in these networks and get a better understanding of the complex communication happening in our brains. Using these techniques, different activity patterns, or oscillations, in different brain areas can be correlated to specific tasks and activities. Studies on large scale brain networks are widely used and have explained important phenomena, from how and when voluntary decisions are made in our brain (Libet, Gleason, Wright, & Pearl, 1983; Soon, Brass, Heinze, & Haynes, 2008), to the brain activity during sleep and its importance (Aeschbach & Borbély, 1993; Huber, Felice Ghilardi, Massimini, & Tononi, 2004).

1.1.3 Sleep

Sleep is an essential part of our lives and we spend approximately one-third of our life asleep. It is crucial to us, but we still do not know much about why. We know that sleep is crucial for learning and memory consolidation (Power, 2004; Walker & Stickgold, 2004), and that sleep deprivation leads to sleep debt, negative health consequences, and changes in emotional responses (Medic, Wille, & Hemels, 2017; Minkel, Htaik, Banks, & Dinges, 2011).

Our sleep cycle can be divided into two main groups; rapid eye movement (REM) and non-rapid eye movement (non-REM). Non-REM sleep can again be divided into 3 stages (1-3), which are distinguished by the cortical activity pattern though EEG. The deepest of these stages, stage 3 (also known as slow-wave sleep), is characterized by slow-wave activity (SWA); high-voltage and low-frequency signals (0,5-4 Hz) (Greene & Frank, 2010). SWA seems to be an important part of the sleeping cycle, as it homeostatically regulated (Bellesi, Riedner, Garcia-Molina, Cirelli, & Tononi, 2014; Dijk, 2009). It has been shown that sleep deprivation can lead to certain cortical neurons firing in an SWA-like pattern, resembling sleep in local areas in the cortex (Vyazovskiy et al., 2011). SWA has been shown to increase over the duration of sleep, and also to increase with sleep deprivation (Bellesi et al., 2014). The non-REM sleep state is considered to be the unconscious state, while the REM stages are considered to be conscious but unresponsive (Sanders, Tononi, Laureys, & Sleigh, 2012). The high amplitude potentials observed in EEG during deep sleep and unconsciousness indicate synchronous activity of cortical neurons, which could increase the impact of the neurons if they converge on a cell. In order to trigger the switch from an asynchronous to a synchronous state and from a conscious to an unconscious state, an ambiguous wide-spread signal has to be sent. A system which is likely to regulate this transition is the modulatory system.

1.1.4 Neuromodulation

Our brains have several mechanisms for regulating synaptic efficacy and neuronal activity, and one of the main systems for this are the modulatory systems. These systems, such as the cholinergic, serotonergic, noradrenergic and dopaminergic, are highly connected throughout the brain and to each other (figure 1.1) (Avery & Krichmar, 2017). Most of these systems have their origin in the reticular formation in the brain stem, and studies have shown that lesion or disruption of regions in or around the reticular formation can alter the

sleep/wakefulness cycle (Camacho-Arroyo, Alvarado, Manjarrez, & Tapia, 1991; Cespuglio, Gomez, Faradji, & Jouvet, 1982; Lindsley, Bowden, & Magoun, 1949; Nitz & Siegel, 1997).

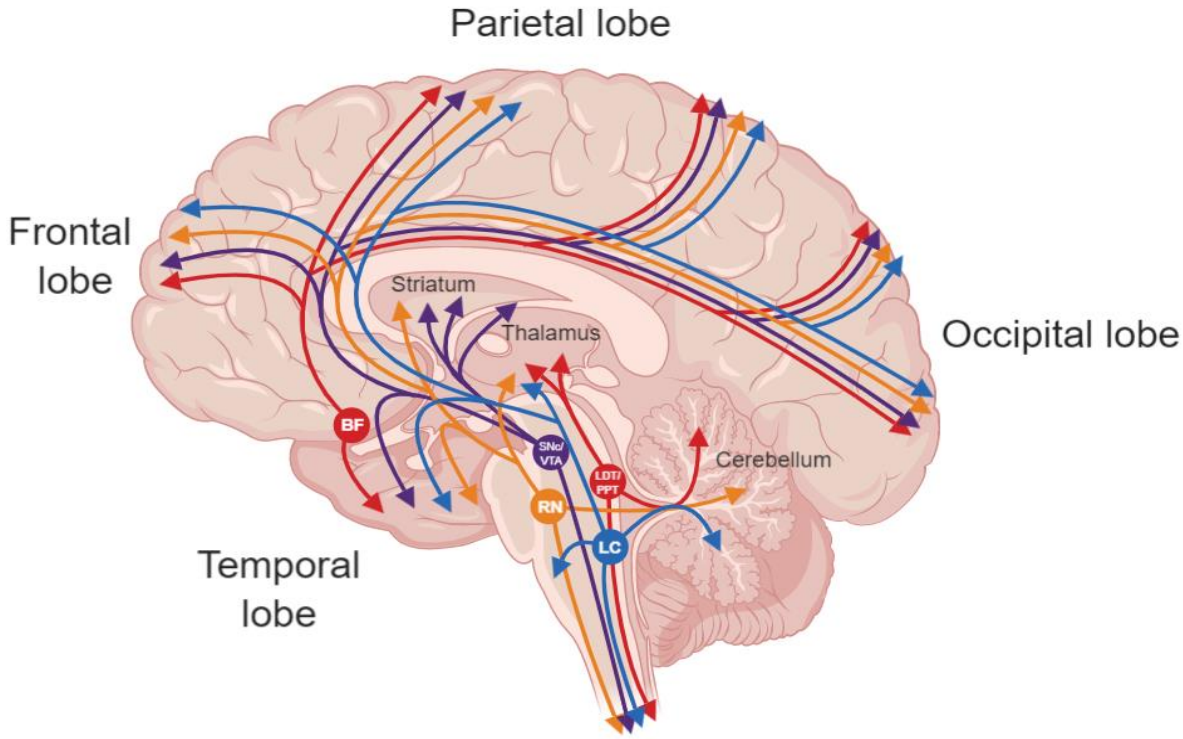

Figure 1.1: A representation of modulatory systems in the human brain. Red shapes represent the cholinergic system, where projections from the basal forebrain (BF), the lateral dorsal tegmental (LDT), and the pedunculopontine (PPT) are illustrated. Purple shapes represent the dopaminergic system, where projections from substansia nigra pars compacta (SNc) and the ventral tegmental area (VTA) are illustrated. The serotonergic system is illustrated with yellow, where projections from raphe nuclei (RN) are illustrated. The blue projections represent the noradrenergic system, with projections from locus coeruleus (LC) represented. Only the largest clusters from each of these modulatory systems were included for simplicity, and the projections are rough representations of the areas innervated by these systems. Figure created with Biorender.com

One reason why these neuromodulators are important for regulating brain states is due to their indirect effect on a cell's firing (Nadim & Bucher, 2014). Neuromodulators can have fast-acting effects through binding to ionotropic channels and directly influencing the conductance of the channels and the membrane potential (Lu & Henderson, 2010), but often have complex slow-acting effects through metabotropic channels, where the effects vary depending on a cells receptors and the intracellular signaling, or even on the concentration of the neuromodulator (Araneda & Andrade, 1991; Collins, Probett, Anson, & McLaughlin, 1984; Gamper, 2016). Many of the synapses from these modulatory centers are considered to transmit through *volume transmission*, where the neuromodulators are released into the extracellular space, affecting an entire neuronal population in the area. (Fuxe et al., 2010; Zoli

et al., 1998). There is evidence for acetylcholine (ACh) receptors even along the axon and on the axon terminal (Abrams et al., 2006; Picciotto, Higley, & Mineur, 2012).

Several neuromodulators are important for regulation of sleep and arousal, including dopamine, noradrenaline, and histamine (Berridge, Schmeichel, & España, 2012; Dzirasa et al., 2006; Thakkar, 2011). One of the more crucial neuromodulatory systems to regulate wakefulness is the cholinergic system (Dzirasa et al., 2006; Steriade, 2004)

1.1.5 Cholinergic modulation of sleep

Acetylcholine is an important neurotransmitter in the peripheral nervous system, where it is the main neurotransmitter at neuromuscular junctions inducing muscle contraction. In the central nervous system (CNS), cholinergic projection neurons originate in the basal forebrain, where cell clusters containing cholinergic somata can be found in the medial septal nucleus, diagonal band of Broca, the nucleus basalis of Meynert, pedunculopontine nucleus, and the laterodorsal tegmental nucleus (M. Marsel Mesulam, Mufson, Levey, & Wainer, 1983; M. M. Mesulam, Mufson, Wainer, & Levey, 1983). Many of these neurons project to the neocortex (M. M. Mesulam et al., 1983), and are important for regulation of cortical activity. High levels of ACh are associated with desynchronization of neocortical activity, high neuronal activity in the neocortex, and with wakefulness, while low levels are associated with synchronization of neocortical activity, lower neuronal activity in the neocortex, and with slow wave sleep (SWS) (Lee, Hassani, Alonso, & Jones, 2005; Marrosu et al., 1995; Ode, Katsumata, Tone, & Ueda, 2017).

A pronounced attribute of ACh is its ability to reduce the sAHP current (I_{sAHP}) in pyramidal cells in both neocortex and hippocampus (Benardo & Prince, 1982; Krnjević, Pumain, & Renaud, 1971; Madison & Nicoll, 1986; McCormick & Prince, 1986). The channels underlying this current are permeable for K^+ and are opened by an increase in intracellular Ca^{2+} concentration, which normally follows an AP or a burst of APs. An increased K^+ current leads to hyperpolarization and lowering of the input resistance, which increases the difficulty for new synaptic inputs to trigger an AP while the channels are open. One theory is that the switch from high-frequency oscillatory activity seen in wakefulness to low-frequency waves during non-REM sleep is mediated by an increase sAHP size, resulting from decreased ACh-levels (Buzsaki et al., 1988; Compte, Sanchez-Vives, McCormick, & Wang, 2003; Sanchez-Vives et al., 2010).

1.1.6 General anesthesia

General anesthetics are important tools not only in a clinical setting but also in research. Induction of unconsciousness, amnesia (loss of memory), and analgesia (loss of pain sensation) is important for surgical procedures, and the mechanisms behind their actions are important to understand these processes. Identifying the molecular targets of these drugs, and understanding how they affect the excitability and synaptic transmission of cells and networks will be an important step in understanding the processes of memory, pain, and consciousness. General anesthesia has several similarities to natural SWS, like the enhancement of cortical low-frequency oscillations, and an overall decrease in cortical activity (E. N. Brown, Lydic, & Schiff, 2010; Pachitariu, Lyamzin, Sahani, & Lesica, 2015). There are many different anesthetics, but the mechanisms of many of them are not that well known. Two of the main molecular targets of most general anesthetics have been identified; the γ-aminobutyric acid A ($GABA_A$) receptor and the N-methyl-D-aspartate receptor (NMDAR). A widely used general anesthetic which is thought to exert it's physiological effects mainly through $GABA_A$ receptor is 2,6-diisopropylphenol, also known as propofol (Feng, Kaye, Kaye, Belani, & Urman, 2017).

1.1.7 Propofol

Propofol has been widely used for induction and maintenance of general anesthesia since its approval in 1989. Propofol is a lipophilic compound mainly known for its potentiation of $GABA_A$ receptors (Hara, Kai, & Ikemoto, 1993; Pittson, Himmel, & MacIver, 2004). Effects on other channels like NMDAR, L-type Ca^{2+} channels, small conductance Ca^{2+}-dependent K^+-channels (SK channels), and HCN channel have also been reported (X. Chen, Shu, & Bayliss, 2005; Funahashi, Mitoh, & Matsuo, 2004; Martella et al., 2005; Orser, Bertlik, Wang, & MacDonald, 1995; Ying & Goldstein, 2005a). Studies on propofol use a range of different concentration, all from 0,1 µM to 1 mM (Kitamura, Marszalec, Yeh, & Narahashi, 2003; Orser et al., 1995). Estimating the free propofol concentration needed in cerebrospinal fluid (CSF) or plasma to induce anesthesia has proven difficult, but several studies have approached this issue. Franks and Lieb (1994) stated that the concentration of propofol in plasma of waking patients was ~1 µg/mL, and assumed that the concentration needed to prevent movement in response to a painful stimulus to be twice that. Combining that with the high protein binding, they calculate the concentration of free propofol in the blood to be

0,4 µM. The doubled value from Franks and Lieb (1994), 2 µg/mL, corresponds with the propofol concentration in plasma during anesthesia found by Engdahl et al. (1998), which they measured to be 2.24 µg/mL. Engdahl et al. (1998) simultaneously monitored propofol concentration in the CSF and measured that to be 0.0355 µg/mL, corresponding to approximately 0,2 µM propofol. In this thesis, a higher propofol concentration (5 µM) than the estimated physiological (<1 µM) was used to elicit stronger and more easily quantifiable responses.

1.1.8 The hippocampus – Its structure and functions

The hippocampus, named for its resemblance to a sea horse, is a structure found in the medial temporal lobe of the cerebral cortex. It can be divided into five subfields; the dentate gyrus, the three subfields of Cornu Ammonis (CA1, CA2, and CA3), and the subiculum. In contrast to the neocortex, the hippocampus is only comprised out of three cell layers; Polymorphic layer, the pyramidal layer, and the molecular layer. The pyramidal layer contains the somata of pyramidal cells, a type of large cells which take their name from their triangle-shaped (pyramidal-shaped) cell bodies. These cells are considered as one of the main output of hippocampus (Bloss et al., 2018), and are therefore the subject of many hippocampal studies on a cellular level.

The hippocampus is mostly known for its importance in episodic memory and learning, and has been a major site for research on memory and plasticity since the famous case of patient H.M. As a result from a bilateral lesion in the hippocampi, H.M suffered from severe retrograde amnesia and partial anterograde amnesia (Scoville & Milner, 1957). In subsequent research, it has also been shown to be an important structure in regards to spatial memory and navigation, with the discovery of place cells (O'Keefe & Dostrovsky, 1971).

1.2 Cellular properties

1.2.1 Up and down states

During SWA, an oscillation in cortical activity can be observed in extracellular recordings. These oscillations are characterized by one phase with the synchronized firing of APs (ON phase) and another phase with synchronized inactivity (OFF phase) (Vyazovskiy et al., 2009).

These alternating periods of activity and inactivity can be observed in individual cells in both *in vivo* and in brain slices, where during ON periods the cell fires bursts of APs, while during OFF periods the cells hyperpolarize (Vyazovskiy & Harris, 2013). The emergence of these ON and OFF periods results from the fact that neocortical neurons have two preferred membrane potentials; a depolarized state (up state) and a hyperpolarized state (down state) (Cowan & Wilson, 1994), a property called bistability. During the up state, the membrane potential is only a few millivolts away from the AP threshold, which increases the sensitivity for synaptic input. During the down state, the membrane potential is relatively hyperpolarized and characterized by the lack of synaptic input (Wilson, 2008).

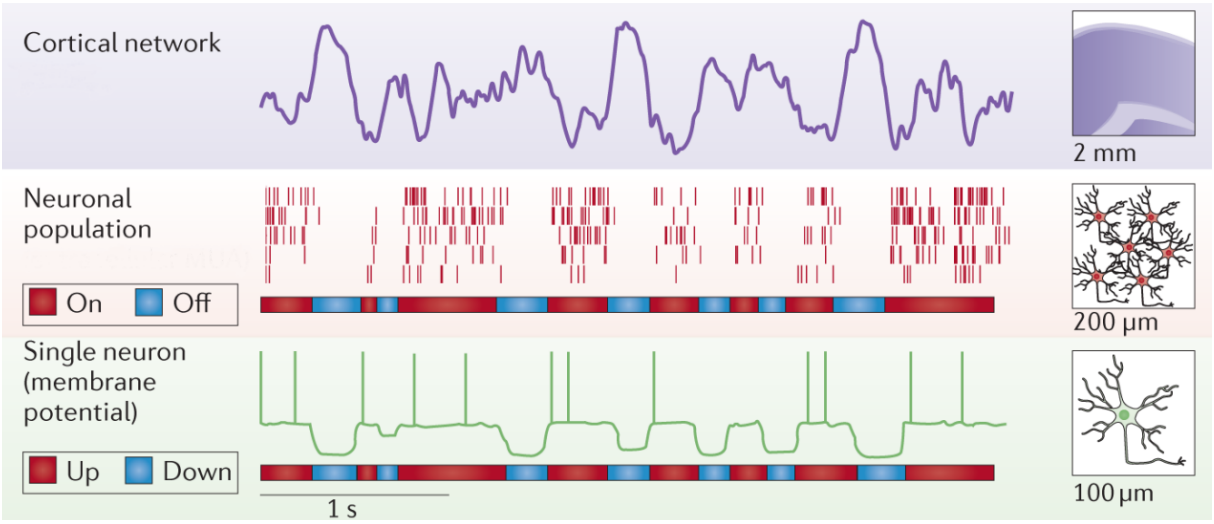

Figure 1.2: SWA during non-REM sleep in rat. Top row shows the slow and high amplitude oscillations produced by synchronous activity. Middle row shows a raster plot of the activity of five cells, where each line represent an action potential. Bottom row shows the membrane potential in an individual cortical neuron, where the neuron is firing action potentials during the up states, before hyperpolarizing to a down state. Figure adapted from "Sleep and the single neuron: the role of global slow oscillations in individual cell rest," by V. Vyazovskiy and K. Harris, 2013, Nature Review Neuroscience.

As mentioned in 1.1.3, SWA appears to be an important aspect of sleeping, as it is homeostatically regulated. SWA is high early in sleep and decreases along with the duration

of sleep, and increases with sleep deprivation (Tobler & Borbély, 1986). One hypothesis is that during OFF periods in SWA when there is no synaptic activity, maintenance and restorative processes can take place (Vyazovskiy & Harris, 2013). The high neuronal activity during wakefulness is believed to lead to several types of cellular stress, such as accumulation of harmful metabolic products as reactive oxygen species and misfolded proteins (Vyazovskiy & Harris, 2013).

As up and down states are important regulators of neuronal and synaptic activity during sleep, many studies have attempted to explain the mechanisms and the currents underlying the states and how a cell transitions from a state to another. One of the factors assumed to be important for the transition from an up state to a down state is the sAHP (Hill & Tononi, 2005), where the accumulation of calcium during the up state is thought to lead to the opening of potassium channels, causing an outward current which helps the cell transition into a hyperpolarized down state. In a Hill and Tononi (2005) *in silico* model, removal of the current underlying sAHP resulted in increased up state duration and reduced down state duration, desynchronization of cortical activity, and an increased oscillation frequency.

1.2.2 Afterhyperpolarization

Afterhyperpolarization (AHP) is the phase after an AP or a series of APs where the membrane potential falls below, or negative to, the resting membrane potential (RMP). AHPs can be divided into three groups based on their durations and their sensitivities to different compounds; a fast afterhyperpolarization (fAHP), lasting usually a few milliseconds, a mAHP, lasting usually a few hundred milliseconds, and a sAHP, which can last up to several seconds (Schwindt, Spain, Foehring, Chubb, & Crill, 1988). These AHPs are important for regulation of excitability and of the spiking properties of neurons, by reducing the probability of reaching the threshold for firing an AP right after activation. AHPs have been reported to play an important role in functions like regulation of learning different hippocampus-dependent tasks (Moyer Jr, Thompson, & Disterhoft, 1996; L. T. Thompson, Moyer, & Disterhoft, 1996), and regulation of the circadian clock (Cloues & Sather, 2003; Whitt, Montgomery, & Meredith, 2016). It has been shown that hippocampus-dependent learning decreases the sAHP in CA1 pyramidal cells, which increases their excitability (Oh, Kuo, Wu, Sametsky, & Disterhoft, 2003). An increase in AHP has also been observed in CA1 pyramidal

cells in aged rats, hypothesized to be the cause behind age-related learning impairment (Matthews, Linardakis, & Disterhoft, 2009; Tombaugh, Rowe, & Rose, 2005).

1.2.3 Slow afterhyperpolarization

The sAHP, which follows a prolonged depolarization, was first described almost 40 years ago and was rapidly identified as a Ca^{2+}-dependent K^+-current. Even though sAHPs have been studied for a few decades now, the K^+ channel responsible for the I_{sAHP} is still unknown (Larsson, 2013). Over the years, several channels have been proposed to play a role in the sAHP. One of the channels investigated was the SK channel (Bond et al., 2004), which has been ruled out in subsequent research. Another proposition for the channel underlying the sAHP in CA1 pyramidal cells, was the intermediate Ca^{2+}-dependent K^+-channel (IK channel) (King et al., 2015), though this has not been without opposition. Other studies have shown that these channels do *not* contribute to sAHP in CA1 pyramidal cells (Wang et al., 2016). Recently, the intracellular Ca^{2+} sensor hippocalcin has been demonstrated to play a crucial role in sAHPs in CA1 pyramidal cells, where a hippocalcin knock-outs have a significantly reduced I_{sAHP} (Tzingounis, Kobayashi, Takamatsu, & Nicoll, 2007).

One of the reasons there has been such interest in sAHP is its highly modifiable nature (Andrade & Nicoll, 1987; Haas & Konnerth, 1983). There are several pathways implied in the modification of sAHP. Noradrenaline, serotonin, dopamine, and histamine seem to reduce sAHP through a cyclic AMP- and protein kinase A-mediated pathway in CA1 pyramidal cells, while ACh is reported to work through a PKA-independent pathway to reduce the sAHP size (Paola Pedarzani & Storm, 1993; P. Pedarzani & Storm, 1995).

There have been reports that the sAHP consists of two components; an early Ca^{2+}-dependent phase and a late Ca^{2+}-independent phase (Schwindt et al., 1988). A study from 2011 showed that the early sAHP phase is modulated primarily by M_1 muscarinic receptors, demonstrating that in M_1 knock-out CA1 pyramidal cells the early sAHP was not decreased as a response to a cholinergic agonist (Dasari & Gulledge, 2011).

1.2.4 Medium afterhyperpolarization

In similarity with the sAHP, there has and still is some controversy regarding the ion channels underlying the mAHP in CA1 pyramidal cells. Studies have shown that mAHP is primarily

dependent on two voltage-gated channels, HCN channel and M-channel, where the M-channel is responsible for mAHP during more depolarized RMPs, and the HCN channel during more hyperpolarized RMPs (Gu, Hu, Vervaeke, & Storm, 2008; Gu, Vervaeke, Hu, & Storm, 2005). Even though Gu et al. (2005, 2008) and others (S. Chen, Benninger, & Yaari, 2014) excluded it, some studies regard the SK channel as an important channel for mAHP and regulation of excitability in CA1 pyramidal cells (Church, Brown, & Marrion, 2019).

The HCN-channel is a voltage-gated channel permeable for K^+ and $Na^{+,}$ which is activated by hyperpolarization, where the voltage-dependent opening of the channel can be regulated by intracellular cyclic AMP levels (Biel, Wahl-Schott, Michalakis, & Zong, 2009). A fraction of HCN channels are open at resting potentials, and therefore have a small depolarizing effect on the RMP (Pape, 1996). Hyperpolarization of the cell will open more HCN channels, which increases the Na^+ conductance and results in a small depolarization which partially counteracts the hyperpolarization. A depolarization of the cell will reduce the number of HCN channels open, decreasing the Na^+ conductance and resulting in a small hyperpolarization.

The M-channel is a voltage-gated channel permeable for K^+ which is activated by depolarization and is, in addition to contributing to the mAHP¤, important for regulating excitability, synaptic integration, and spiking (Hu, Vervaeke, & Storm, 2007). Similarly to HCN channels, a fraction of M-channels are also open at resting potentials, and the K^+ conductance of these channels drive the RMP to a more hyperpolarized value (Petrovic et al., 2012). When a cell depolarizes, more M-channels open, increasing the K^+ conductance and partially counteracting the depolarization. M-channels are targets for different modulations, such as M_1 muscarinic receptor-mediated inhibition (D. A. Brown & Passmore, 2009).

1.2.5 Synaptic transmission

Efficacious synaptic transmission is crucial in neuronal networks, as it is the main form of communication between neurons. This process is highly plastic and is the target of many different types of modulation. Different processes like the neurotransmitter release, binding to receptors, and conductance of ion channels and integration of the postsynaptic potentials can be modulated (Froemke, Poo, & Dan, 2005; Lovinger, 2010; Monaghan, Irvine, Costa, Fang, & Jane, 2012).

One of the first discovered forms of synaptic modulations was the long-term potentiation (LTP) (Bliss & Lomo, 1973; Collingridge, Kehl, & McLennan, 1983; McNaughton, Douglas, & Goddard, 1978). A key component in many types of LTPs is the NMDAR. NMDAR is an ionotropic channel, which is normally blocked by a Mg^{2+} or a Zn^{2+}. The opening of this channel not only requires both glutamate and glycine but also a strong enough postsynaptic depolarization for the divalent ions to be displaced. This can happen through high synaptic stimulation or through spike-timing-dependent plasticity, where a backpropagating AP coincides with synaptic activity (Markram, Lübke, Frotscher, & Sakmann, 1997). LTP can increase synaptic efficacy through several different mechanisms like the insertion of new α-amino-3-hydroxy-5-methylisoxazole-4-propionic acid receptors (AMPARs), or through phosphorylation of AMPARs which can increase their conductance (Lüscher & Malenka, 2012; Shi et al., 1999). As synaptic efficacy can increase through activity-dependent mechanisms, it can also decrease. Low-frequency stimulation may lead to a process called long-term depression, where the synaptic efficacy is decreased (Bear & Malenka, 1994).

A cell's response to synaptic activity depends on several factors. The dendrites are active compartments, containing voltage-gated channels important for integration and processing of postsynaptic potentials (Cai et al., 2004; Magee & Johnston, 2005). Two of the important voltage-gated channels for modulation of synaptic potentials in the dendrites are the HCN channels and the M-channels. In response to depolarization, HCN channels will close and M-channels will open, resulting in a decreased Na^+ conductance and an increased K^+ conductance, respectively. Due to the slow opening and closing kinetics of HCN channels and M-channels, these changes in currents will mostly affect the peak and the repolarization phase of the EPSPs. HCN channel closing due to a depolarizing postsynaptic potential results in a faster decay of the EPSPs, reducing the temporal summation (Magee, 1999). M-channel opening increases with increasing depolarization and will inhibit larger EPSPs to a greater extent than smaller EPSP (Hu et al., 2007).

1.3 Aims of the study

SWA is enhanced during general anesthesia, where large oscillations representing the up and down states in cortical cells are seen. Hill and Tononi (2005) presented an important role for I_{sAHP} in their model of SWA. Here, I_{sAHP} is the main factor in the termination of the up state and plays an important part in the synchronization of firing.

- The main purpose of the study is to determine propofol's effect on sAHP in CA1 pyramidal cells, and if the formation of SWA during general anesthesia could be explained by a modification of sAHP size.
- Secondary goals are to determine if and how propofol synaptic transmission from perforant path fibers to the soma, and determine propofol's effect on mAHP in CA1 pyramidal cells.

There are several reasons for choosing the hippocampal CA1 pyramidal cells as a model. Hippocampus has been frequently used in different studies in this research group, and the protocols are well established. The vast amount of research done on the hippocampus and on CA1 pyramidal cells worldwide provides solid background knowledge about the channel expression in these cells and their properties. Insight into how these cells process information and how these processes are modulated are important for potentially explaining the observations. In addition, the hippocampus was chosen for its simplicity. In contrast to the neocortex, CA1 of hippocampus only contain one pyramidal cell layer. This makes it easier to identify and consistently record from the same cells.

2 Materials and methods

2.1 Ethical approvals

All experimental procedures were performed in line with the guidelines set by the responsible veterinarian at the Institute of Basic Medical Science, University of Oslo, and in accordance to the statute regulating animal experimentation given by the Norwegian Ministry of Agriculture, 1996. All participants involved in these experiments had the FELASA (Federation for Laboratory Animal Science Associations) certificate required by the Norwegian Food and Safety Authority to perform animal research.

2.2 Animal housing

Male Wistar rats (Scanbur, Denmark) were kept in the local animal facility and under a 12-hour light/dark cycle, with lights on from 07.00 to 19.00. The animals were housed in GR900 cages with a floor area of 904 cm^2, with *ad libitum* food and water. The temperature was kept at ~23°C, the relative humidity at 55%, and the air exchanged 65 times per hour.

2.3 Experimental setup

The recording chamber was mounted on a BX51WI (Olympus, Tokyo, Japan), an infra-red difference interference contrast microscope, using 10x and 60x lenses. A VX55 infra-red camera (TILL Photonics, Gräfelfing, Germany) mounted on top of the microscope was connected to a screen for visualization. Inflow and outflow tubes were placed on opposite sides of the recording chamber, along with a ground electrode and thermometer sensor wire. A heating unit around the silicone inflow tube was used to regulate the bath temperature.

Two micromanipulators (Luigs & Neumann, Ratingen, Germany) mounted to the anti-vibration table were used for the controlled and precise movement of the recording and stimulation pipettes. Air pressure in the recording pipette was regulated through the application of positive pressure or suction and opening or closing a three-way valve.

The entire experimental setup was mounted on an anti-vibration table to minimize any vibrations in the ground, and placed within a Faraday cage to reduce external electrical noise.

2.4 Slice preparation

Transverse hippocampal slices were made from young male Wistar rats (days 21-28 postnatal) using a Leica VT1200 semiautomatic vibrating blade microtome (Leica Biosystems Inc., Buffalo Grove, IL, USA). Rats were deeply anesthetized in Suprane (Baxter Medical AB SE, Kista, Sweden) before decapitation. The brain was removed and submerged in ice-cold cutting solution (see appendix 5.2.1, table 5.2), which was saturated with carbogen (95% O_2/5% CO_2), for about one minute. The cerebellum and about 0,5 cm of the frontal part of the brain were then cut off, and the remainder was then fixed to a specimen plate using super glue. The specimen plate was placed in an ice-cold metal buffer tray, which was then filled up with a pre-chilled cutting solution to submerge the brain. The buffer tray containing the brain was placed inside an ice tray filled with ice and locked in place onto the vibratome. Slices were cut 400 µm thick and transferred to a chamber filled with artificial cerebrospinal fluid (aCSF) (see appendix 5.2.2, table 5.4) and placed in a water bath at ~35°C for 30 minutes to recover from the stress of the slicing procedure. After the 30 minutes, the chamber was kept at room temperature (20-25°C).

2.5 Electrophysiology

Whole-cell current clamp recordings were performed in aCSF saturated with carbogen and held at temperatures 30-33°C. For whole-cell recordings, patch pipettes were pulled using a PP-830 vertical pipette puller (Narishige, Tokyo, Japan) from borosilicate glass capillaries (Sutter Instrument, Novato, CA, USA) with an outer diameter of 1,5 mm and an inner diameter of 0,86 mm. Patch pipettes were filled with an intracellular solution (see appendix 5.2.3, table 5.5).

Recordings were acquired from CA1 pyramidal cell somata, which were visually identified. Once the patch pipette was in the bath, the amplifier was switched to voltage-clamp settings and the membrane test protocol was initiated to measure the resistance of the pipette. Pipettes with lower resistance than 3 MΩ or higher than 8 MΩ were discarded. The pipette was then brought towards the slice, and small positive pressure was applied. As the pipette was in close proximation of a target pyramidal cell, positive pressure was released, and suction was applied. To increase the chances of getting a good seal, the holding potential was decreased to approximately -70 mV. When a giga-ohm seal was established (the resistance between the

pipette tip and the ground electrode in the bath reached 1 GΩ), the continuous suction was relieved. Sharp and short suction was instead applied to rupture the cell membrane at the tip of the pipette and break into the cell. Cells with an unstable RMP, unstable seal, or an unstable input resistance were discarded. The RMP was held at -65 mV in all experiments by adjusting the holding current.

Current-clamp experiments were recorded using a Digidata 1440A digitizer (Molecular Devices LLC, San Jose, CA, USA) and a Dagan BVC-700A amplifier (Dagan Corporation, Minneapolis, MN, USA). The signal was filtered at 10 kHz and digitized at 50 kHz.

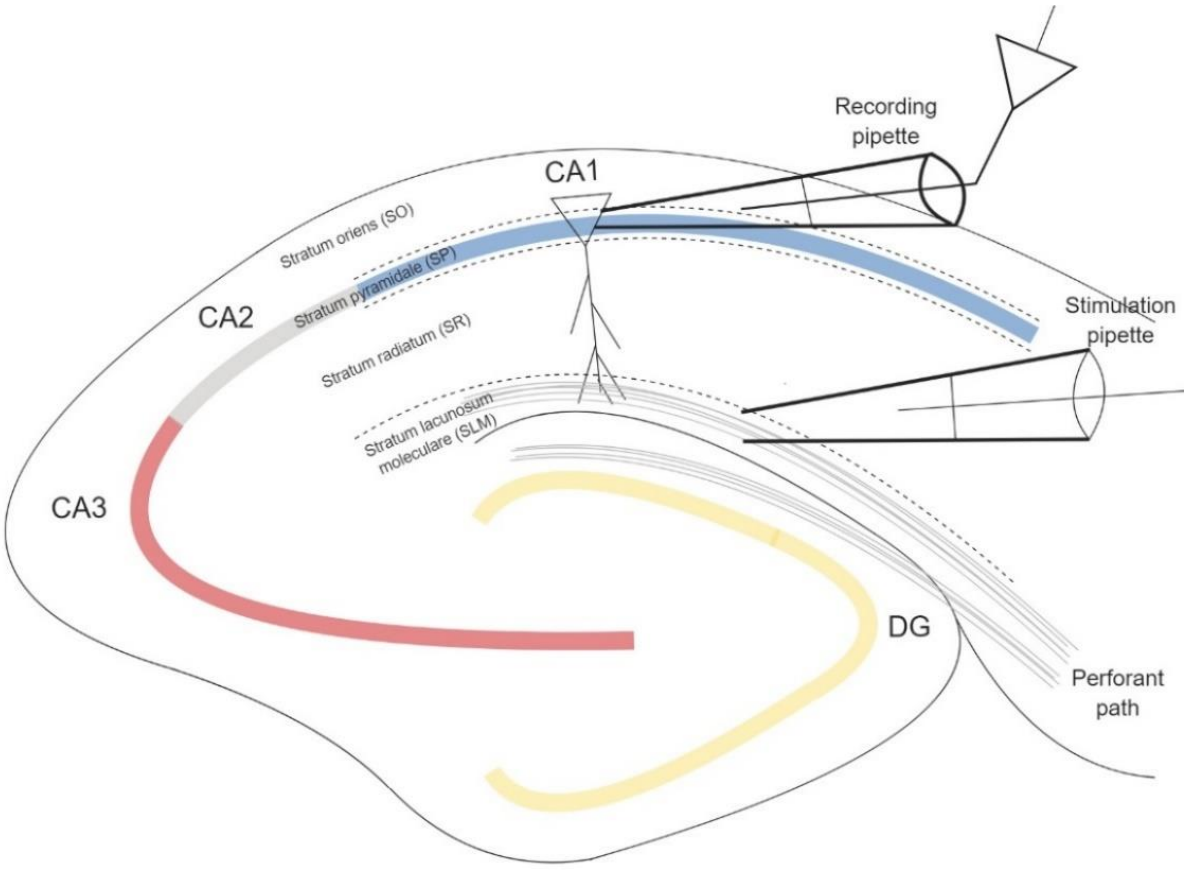

Figure 2.1: Experimental setup in transverse hippocampal slices. The different colored lines illustrate the pyramidal cell layer of the different subfields of the hippocampus. Different regions of the hippocampus are divided by dotted lines. Whole-cell recordings were obtained from CA1 pyramidal cells, which have large and visually identifiable apical dendrites. These apical dendrites have branches which stretch into the stratum lacunosum-moleculare (SLM). Perforant path fibers from layer II medial entorhinal cortex innervate the apical dendrites of CA1 pyramidal cells in the SLM. Figure created with Biorender.com

2.5.1 Extracellular stimulation

Postsynaptic potentials were elicited by extracellular stimulation of the perforant path, achieved by placing a micropipette filled with 1 M NaCl in the lacunosum-moleculare (SLM). Pipettes were pulled by the PP-830 vertical puller from borosilicate glass capillaries with an outer diameter of 1,5 mm and an inner diameter of 0,6 mm, and the tip was visually estimated to be approximately 5 µm in diameter. Pipettes were placed in the SLM. Current pulses were generated by using an isolated stimulator (Hi-Med HG203, London, UK). Extracellular stimulation was either elicited as pulse trains or paired pulses. The pulse trains contained 5 pulses delivered at 50 Hz, with approximately 21 seconds between pulse trains. Paired pulses contain 2 pulses at 10 Hz, with the same interval between.

2.5.2 Liquid junction potentials

When two fluids of different ionic composition, or an electrode and a fluid, come in contact with each other, an electric potential can develop in the interface between these two. To reduce this potential and minimize fluctuations in the measurements, the silver recording electrode was coated with chloride. The presented values in this thesis have not been corrected for the liquid junction potential.

2.6 Drug application

A continuous flow of carbogen saturated aCSF across the slice achieved by using a peristaltic pump. The flow speed was measured to 1,5 mL/min, and the time from the container into the bath was measured to 1 minute and 8 seconds.

SR-95531 (Gabazine) (Tocris, Abingdon, UK), a $GABA_A$ receptor antagonist, was stored in 50 µL aliquots in a -18°C freezer, and diluted in 200 mL aCSF to a concentration of 5 µM gabazine. This was done no later than 30 minutes prior to experiments to ensure that gabazine has circulated through the entire system and that the concentration was uniform.

Propofol, which is a hydrophobic substance, was stored as an emulsion (Lipuro®) containing soybean oil, triglycerides, glycerol, egg lecithin, sodium oleate, and water. The vials containing the propofol emulsion were stored in a +4°C refrigerator. The vials were carefully shaken before use, and propofol was added to a separate container with aCSF (and gabazine if

used) 10 minutes before washing in. Each vial was used for up to two weeks and then disposed of, to avoid contamination and oxidation.

2.7 Data analysis

Data was acquired by using Clampex 10.7 (Molecular Devices LLC, San Jose, CA, USA). For data analysis and statistical analysis, Clampfit 10.7 (Molecular Devices LLC, San Jose, CA, USA) and Origin version 2017 (OriginLab Corporation, Northampton, MA, USA) were used.

2.7.1 Measurement of input resistance

During the time course, five 200 ms negative square current pulses were injected at a frequency of 2,5 Hz. The current was adjusted for each cell, eliciting membrane hyperpolarization of ~5 mV for each pulse. 100 ms before each pulse was used as baseline and the mean value of the last 100 ms of each pulse was used as the change in membrane potential (ΔV) to avoid including capacitive currents. The input resistance was then calculated using Ohm's law;

$$Input\ resistance\ (in\ M\Omega) = \frac{\Delta V\ (in\ mV)}{Size\ of\ currrent\ pulse\ (in\ pA)} \times 1000 \qquad (1)$$

The calculated input resistance values from the five current pulses in the same sweep were then averaged to give the final used value.

2.7.2 Measurement of afterhyperpolarization

mAHPs are usually short-lasting, and peak within a few hundred milliseconds after a positive square current pulse. 100 ms before the current pulse was used as a baseline value, and the peak negative value between 0 and 300 ms after the current pulse was used as a value for mAHP amplitude.

sAHPs can last up to several seconds. For the quantification of sAHPs, the area between 300 ms and 1000 ms after the square current pulse was measured. 300 ms after the current pulse, there should not be much mAHP current (I_{mAHP}) and the sAHP should be large, so any changes in I_{sAHP} would be easily observable.

Both experiments with gabazine and without gabazine have been combined, as there is no evidence for gabazine having any effect on AHP.

2.7.3 Measurement of paired pulses

Changes in paired pulses facilitation often indicate a presynaptic modulation, due to changes in short-term plasticity in the presynaptic terminal (Fioravante & Regehr, 2011). To only measure the excitatory component of the synaptic potentials, and to avoid including a possible effect of temporal summation on the second pulse, the rise slope of both pulses were measured. The rise slope of EPSPs should be minimally influenced by IPSPs, and should also not be largely affected by a few mV differences in the baseline. The measurements were done in Clampfit, and the software calculated the rise slope using the following formula:

$$Rise\ slope\ = \frac{\left(Peak\ positive\ value\ (mV) - Peak\ negative\ value\ (mV)\right) \times 0.8}{(time\ of\ 90\%\ of\ positive\ peak - time\ of\ 10\%\ of\ positive\ peak)} \quad (2)$$

This value represents the rate of change in membrane potential between 10% and 90% of the measured peak.

The paired pulse ratio is then calculated by dividing the rise slopes of the second pulse by the rise slopes of the first.

2.7.4 Measurement of the sag and overshoot

M-channels and HCN channels are both voltage-dependent ion channels with slow opening- and closing kinetics. If a cell is presented with a rapid change in membrane potential, like an injected current step, the channels require some time to open and counter-act these voltage changes, resulting in a sag or an overshoot, due to HCN channels and M-channels, respectively. In both instances, the peak value during the first 200 ms of the current step was used as the peak value, while the mean of the last 100 ms was as the steady-state value.

$$Sag\ or\ overshoot = peak\ value - \text{steady state value} \quad (3)$$

3 Results

Following results are from 18 different cells, where 11 are in the presence of gabazine (+gabazine) and 7 in the absence of gabazine (-gabazine).

The RMP was manually held at -65 mV (unless specified otherwise) by adjusting the holding current throughout the entire recording.

In time course graphs, the x-axis is adjusted, where time = 0 min corresponds to the time of wash-in with 5 µM propofol. The time from wash-in to the arrival of propofol to the recording bath was measured to be 1 minute and 8 seconds.

Results are also presented as box charts, where the “box” represents the interquartile range, containing the middle 50% of all data points. The black line in the box represents the mean, while the error bars represent 1,5 × the interquartile range. Any data points outside that are marked as (•)and are classified as outliers. One single data point represents the average value acquired from one cell.

Statistical hypothesis testing was performed using pair-sample t test. The degree of statistical significance is denoted by asterisks where;

Not significant (n.s.) = $p > 0.05$

* = $p < 0.05$

** = $p < 0.01$

*** = $p < 0.001$

All error bars, excluding box charts, represent the standard error of the mean (SEM).

3.1 Afterhyperpolarization

sAHP have been proposed to play an important role in the formation in large-amplitude and low-frequency cortical oscillations that can be detected by EEG during SWS and anesthesia (as mentioned in 1.1.5). By performing whole-cell patch clamp recording on CA1 pyramidal cells, one can observe the effects of an anesthetic, such as propofol, on electrical properties like AHP. 18 cells were recorded for >1 hour, where the effect of propofol was observed over time. Figure 3.1 (top) illustrates an example trace with an AHP after injection of a 250 ms positive square current pulse. Pulse amplitude was manually adjusted throughout the recording to elicit eight spikes, where the lowest current used was 216 pA and the highest was 745 pA in all cells. Average current to elicit eight spikes is shown in the appendix (figure

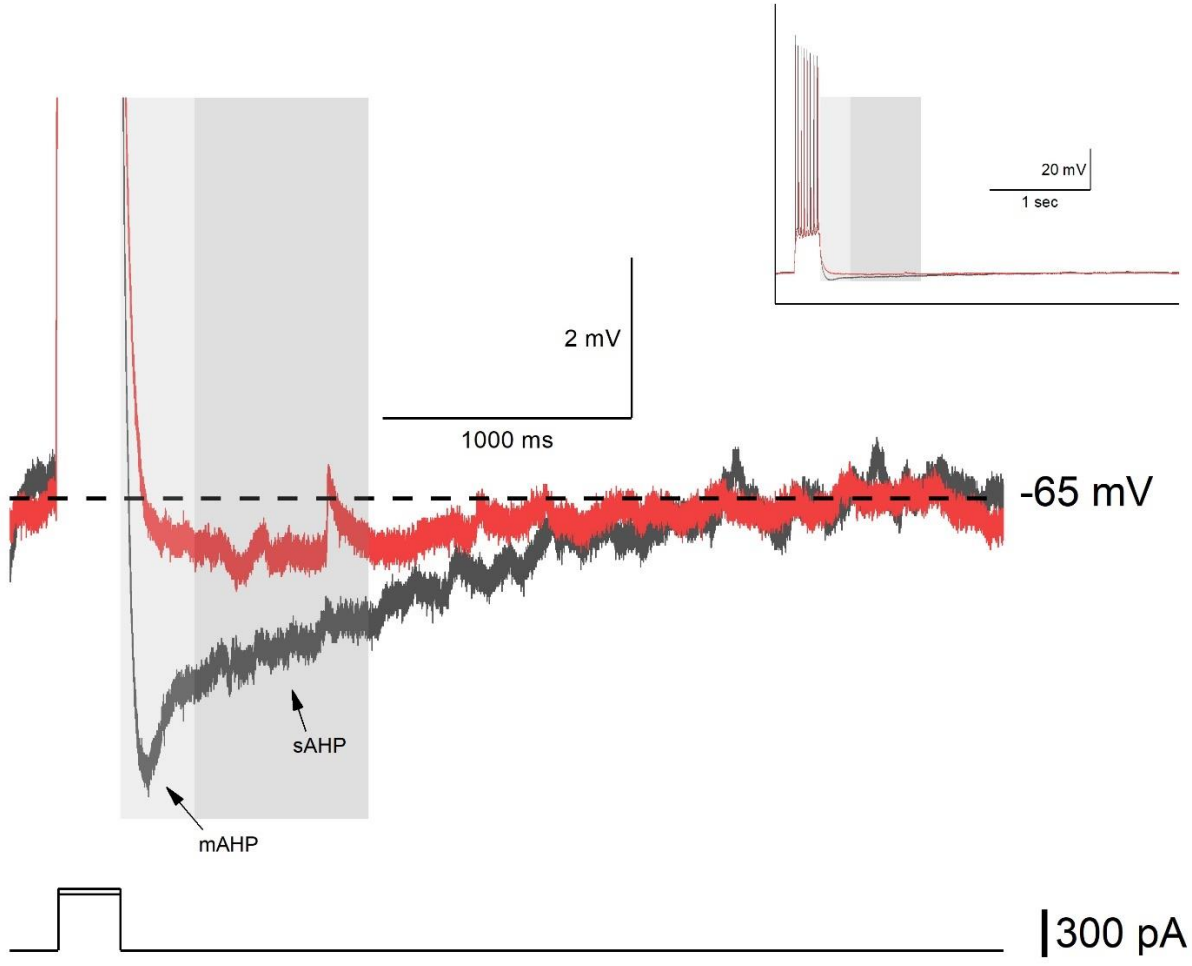

Figure 1.1: Effect of propofol on hyperpolarization. Top graph shows an example voltage trace of the change in afterhyperpolarization in a CA1 pyramidal cell, where the traces are truncated for a clearer view of the hyperpolarization. The black trace is an average of the baseline recordings, while the red trace is after wash-in with propofol. Inset in top right shows the full spike amplitude. The dotted line represents the membrane potential before the depolarization. Bottom graph shows the square current pulses used to evoke the depolarizations.

5.2). As mentioned in 2.5.3, the first 300 ms after the depolarization were used to analyze the mAHP, represented by the light gray box, from which the peak negative value was used. The next 700 ms were used to analyze the sAHP, where the area in the dark grey box below the dotted line was measured. An evident decrease in both mAHP and sAHP size can be observed in this example.

3.1.1 Slow afterhyperpolarization

As mentioned in 1.1.5 and 1.2.2, the sAHP is an important mechanism for regulation of excitability and is hypothesized to play an important role in producing low-frequency oscillations in the neocortex seen during SWS and anesthesia. Figure 3.1 shows a decrease in sAHP size in a 5 µM propofol-treated CA1 pyramidal cell. To explore this observed change further, the change in sAHP size over time has been plotted. 250 ms current steps of varying

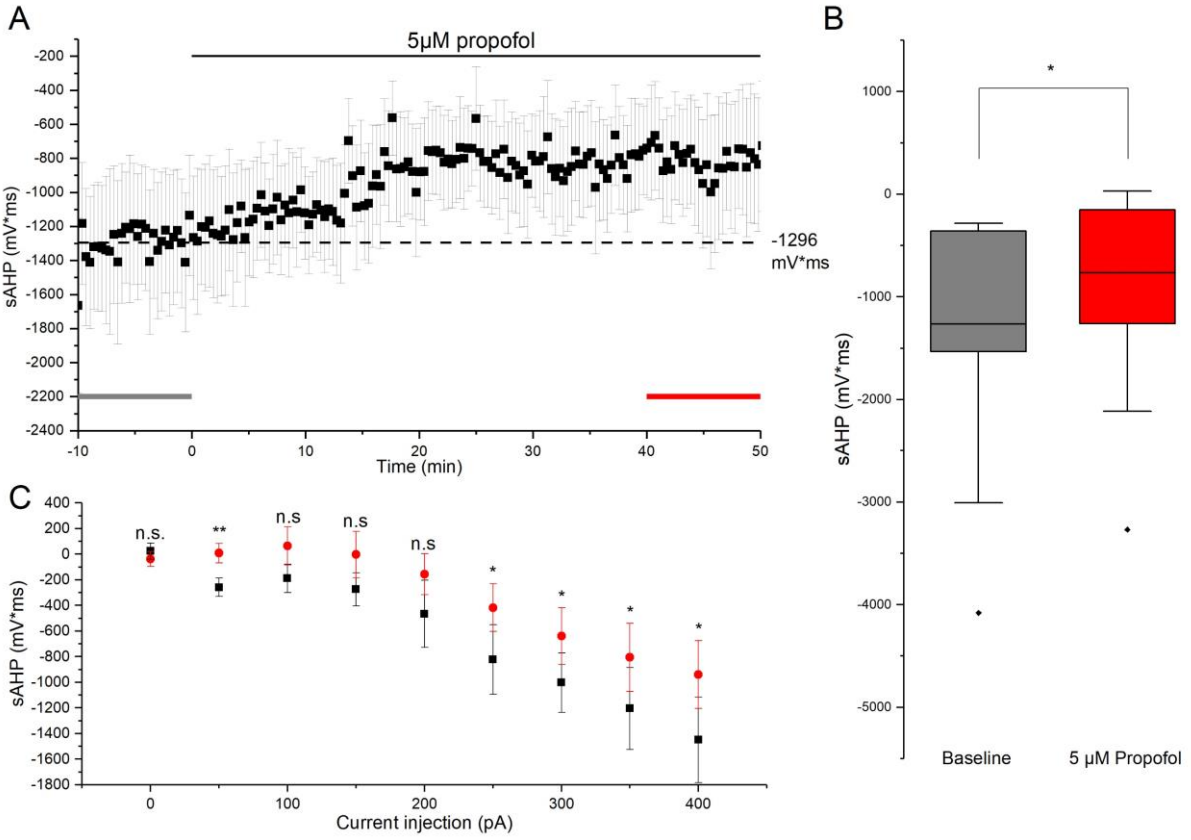

Figure 3.2: Effects of propofol on the sAHP. **A)** Time course of change in sAHP amplitude. Dotted line indicates the average baseline sAHP size (n=11). Grey and red bars represent the time interval analyzed in figure B. **B)** Box chart representing the sAHP size before and after application of 5 µM propofol (p=0,01762, n=11). **C)** Size of sAHP as a function of current injection. 1 second long current steps with 50 pA increments were injected (0 pA – 400 pA), where the changes in size at 50, 250, 300, 350 and 400 pA were significant (n=11).

sizes were used throughout the time course, manually adjusted to evoke 8 spikes. Traces containing more or fewer than 8 spikes were excluded from figure 3.2A and B. Additionally, cells without a clear sAHP at the beginning of the recording, or that did not complete all protocols used to present the data in figure 3.2, were excluded.

Figure 3.2A shows the change in size for 50 minutes after wash-in with 5 µM propofol, after a 10 minute baseline period. The sAHP size seems to decrease after wash-in of propofol, and stabilize approximately 20 minutes after wash-in. The sAHP size of during the first and last 10 minutes of the time course are compared in figure 3.2B. A significant change in sAHP amplitude was observed, where the mean (±SEM) decreased from -1296±398,2 mV×ms during baseline to -814,4±362,8 mV×ms following the addition of propofol, corresponding to a 37,16% decrease in size ($p=0,01762$, $n=11$). A decrease in sAHP size was observed in 10 out of the 11 cells. To test whether this change was dependent on stimulus intensity, current steps of different sizes (0 – 400 pA, 50 pA increments) were injected (figure 3.2C). A significant difference in sAHP size was observed at several current sizes (50 pA: $p=0,00237$, 250 pA: $p=0,03853$, 300 pA: $p=0,02642$, 350 pA: $p= 0,04942$, 400 pA: $p=0,04509$, $n=11$). High inter-sample variability in the 11 cells used for the analysis, resulted in large SEMs.

3.1.2 Medium afterhyperpolarization

Similarly to sAHP, the mAHP is important for spike-frequency adaption. To study the effects of propofol on mAHP, the change in mAHP over time has been plotted in figure 3.3A. Depolarizations were evoked by injection of 250 ms current steps of varying size, manually adjusted to evoke 8 spikes. Traces that did not contain 8 spikes were excluded from figure 3.3A and B. Figure 3.2A shows a clear decrease in mAHP amplitude, seemingly decreasing as a result of the application of 5 µM propofol. All 16 cells used in these analyses had a clear mAHP during the baseline recording, and a decrease in mAHP amplitude could be observed in all 16 cells. The mAHP amplitude during baseline (minute -10 to minute 0) and at the end of the recording (minute 40 to minute 50) was plotted as a box chart in 3.3A. A significant decrease from -2,908±0,3707 mV during baseline to -1,574 mV±0,3613 mV after addition of propofol could be observed, corresponding to a 45,87% decrease ($p=3,98497\times10^{-6}$, $n=16$). To test whether this significant change in mAHP amplitude was only present under conditions used during the time course, different holding potentials (3.3C left) and current injection sizes (3.3C right) were tested. The decrease in mAHP amplitude during different holding potentials

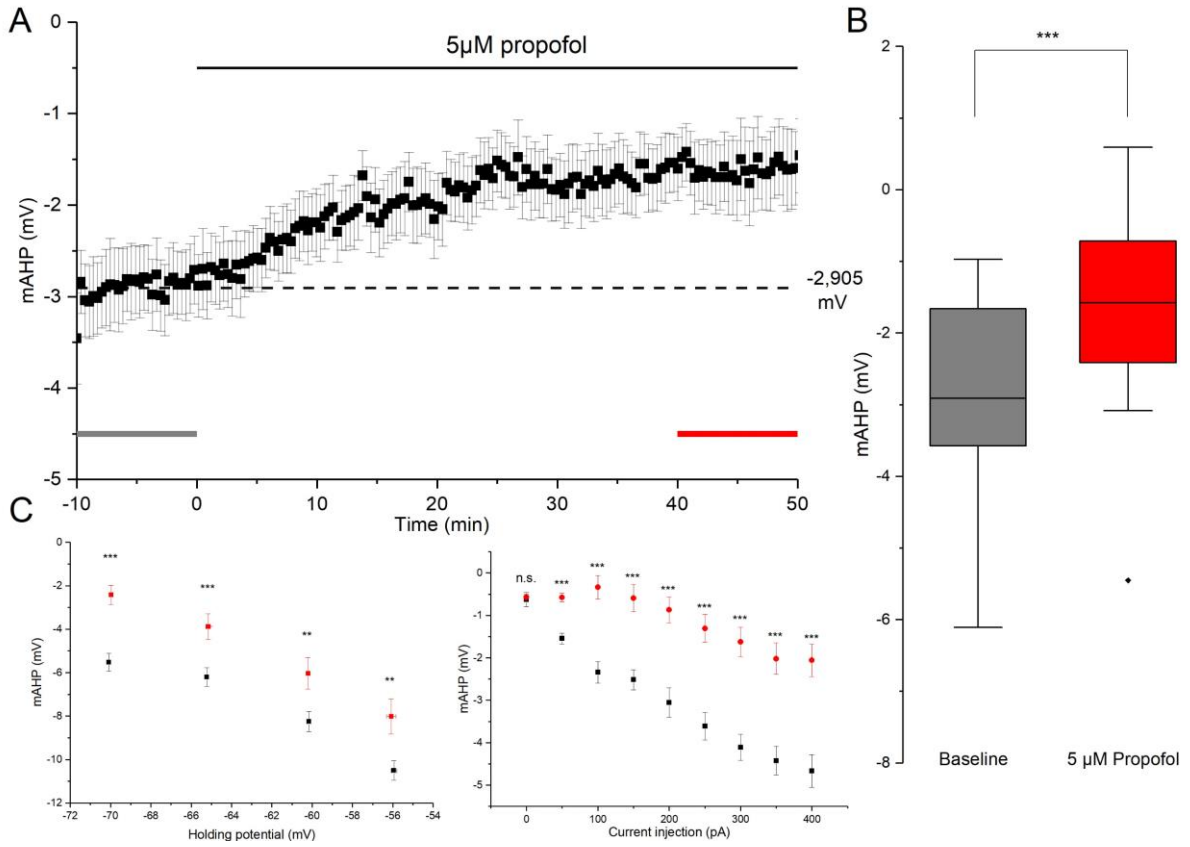

Figure 3.3: Effects of propofol on the mAHP. **A)** Time course of change in mAHP amplitude relative to baseline. Dotted line represents average baseline mAHP peak value (n=16). Grey and red bars represent the time interval analyzed in figure B. **B)** Box chart representing the mAHP amplitude before and after application of 5 µM propofol (p= 3,98497×10^{-6}, n=16). **C)** mAHP amplitude as a function of holding membrane potential (left) and current injection (right). All changes, except the negative control (Injected current = 0 pA), are statistically significant (n=16).

were all significant (-70 mV: p=2,080×10^{-5}, -65 mV: p=5,959×10^{-4}, -60 mV: p=0,00327, -55 mV: p=0,00497, n=16). The decrease was also significant at all current injections tested except at 0 pA (0 pA: p= 0,75506, 50 pA: p= 9,805×10^{-6}, 100 pA: p= 1,016×10^{-4}, 150 pA: p= 2,016×10^{-5}, 200 pA: p=2,058×10^{-5}, 250 pA: p=6,117×10^{-6}, 300 pA: p=1,225×10^{-6}, 350 pA: p=1,142×10^{-5}, 400 pA: 5,27845×10^{-6}, n=16). Though the change seems to be independent of stimulus intensity, a change in the pattern can be observed in figure 3.3C (right). During the baseline recording, the relationship between current size and mAHP amplitude seemed to be close to linear. After wash-in with propofol, this pattern seemed to change for the smallest currents used, where the mAHP did not increase from a current step of 0 pA to a current step of 150 pA (0 pA, propofol: -0,5913±0,3183 mV, 150 pA, propofol: -0,5732±0,07091 mV). A possible explanation for this will be discussed in 4.2.2.

3.2 Channels underlying mAHP

3.2.1 HCN channels

To determine the molecular target of propofol which causes the change in mAHP amplitude, one has to look at the possible candidates. One of the channels known to mediate the mAHP in CA1 pyramidal cells is the HCN channel. When a negative current step is injected, the initial hyperpolarization will be followed by a small depolarization. This delayed depolarization, called the sag, is due to the slow opening of HCN channels, which increases the conductance for Na^+ and brings the membrane potential to a more depolarized potential. The sag is easily quantifiable and is represented in figure 3.4A (top) by the two dotted lines. Figure 3.4A (top) shows an example trace from before and after 5 µM propofol was washed in is presented. The baseline trace (black) is a result of a 1 second -300 pA current injection, while the propofol trace (red) is a result of a -250 pA current injection as illustrated in the

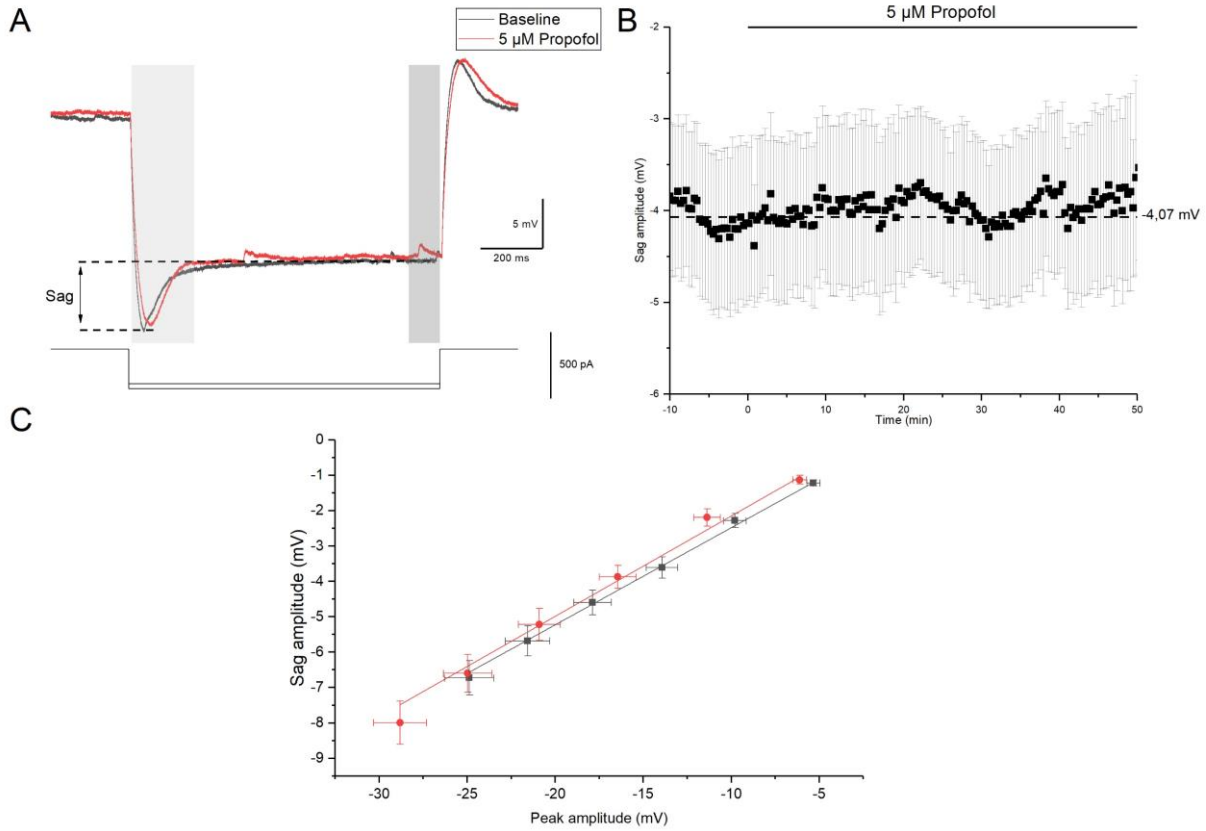

Figure 3.2: HCN channel activity. **A)** Example traces of the sag from the same cell before (black trace) and after 5 µM propofol (red trace) after wash-in. Bottom trace shows the current pulses. **B)** Time course of the average sag amplitude (n=17). Dotted line represents the average baseline sag amplitude. **C)** Sag amplitude as a function of peak depolarization, with averages from before (black) and after (red) wash-in with 5 µM propofol (n=17). Current steps with 50 pA increments (-300 to -50 pA) were used. Data has been linearly fitted.

bottom graph. As the input resistance increased after application of propofol (see appendix 5.1, figure 5.1), a lower current step was required to elicit the same hyperpolarization. These traces were chosen due to a similar resting potential and similar steady-state potential, making them easier to compare visually. The light gray box represents the area used to measure the peak amplitude, while the dark gray box represents the area used to measure the "steady-state" mean value.

During the time course, a 1 second -200 pA hyperpolarizing current was injected. The change in sag amplitude over time is plotted in figure 3.4B. One cell was not included as it did not complete the protocols used in figure 3.4.

Since the HCN channel is voltage-dependent, the channel activity, and thus the sag amplitude, will depend on the size of the hyperpolarization. And since the input resistance increased (see appendix 5.2.1, figure 5.1), studying the change in sag amplitude over time could give an incorrect representation of the change. By plotting the sag amplitude as a function of the peak hyperpolarization, an input resistance-independent and more accurate representation of the HCN channel activity can be made. This is plotted in figure 3.4C and linearly fitted to illustrate the HCN channel activity at different membrane potentials. No change in the pattern of activity of HCN channels can be observed.

3.2.2 M-channels

The second channel which is widely accepted to be an important component of the mAHP is the M-channel. M-channels are activated by depolarization and are permeable to K^+. One method to investigate M-channel activity is to look at subthreshold depolarization, where depolarizations will produce a "reverse sag" (Gu et al., 2005). The reverse sag (overshoot) is a small hyperpolarization in the initial part of a depolarizing step, due to the opening of voltage-gated M-channels. The opening of these channels results in an increased K^+ conductance, reducing the membrane potential to a more negative value. The overshoot is represented by the two dotted lines in figure 3.5A. Figure 3.5A (top) shows an example trace of a cells response to a 1 second, 50 pA current step. The light gray box represents the area used to measure the peak amplitude, while the dark gray box represents the area used to measure the "steady-state" mean value. In the baseline example trace, there is a clear overshoot period approximately 100 ms after the beginning of the current step, before stabilizing at ~1 mV

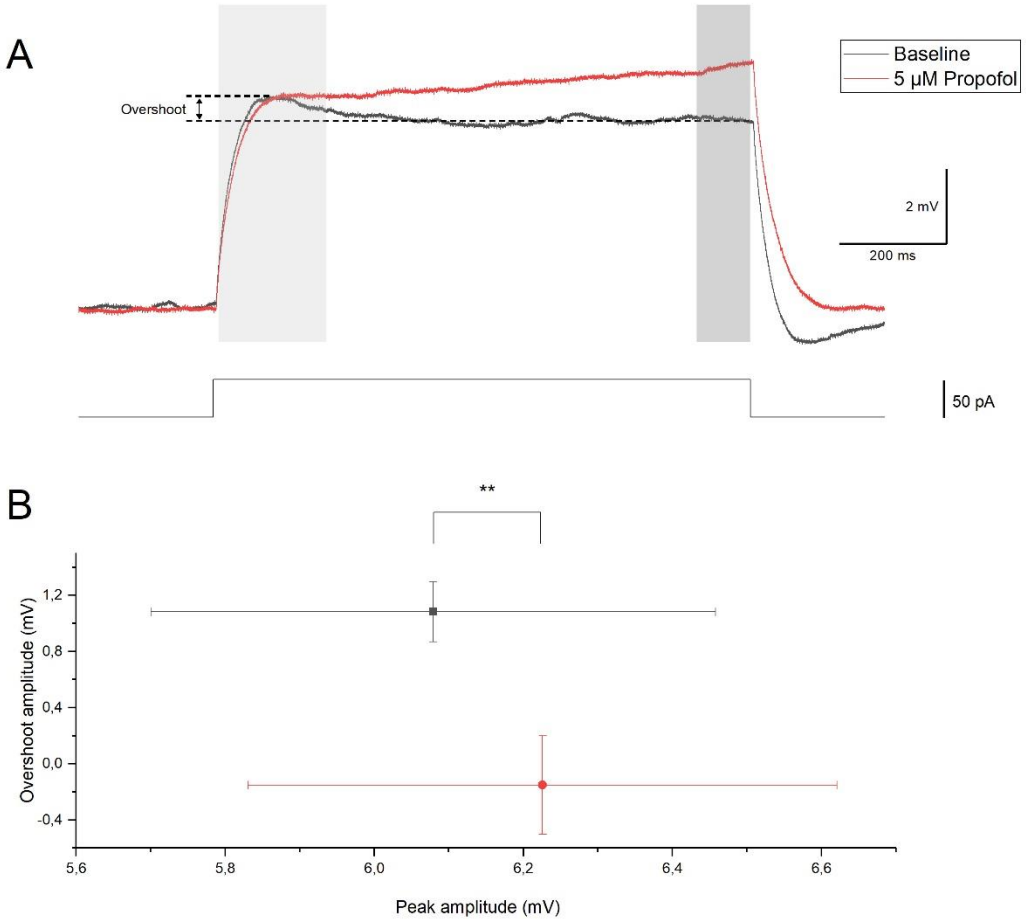

Figure 3.5: Overshoot in a subthreshold depolarizing step. **A)** Example trace of a subthreshold depolarizing step in the same cell before (black) and after (red) wash-in with 5 µM propofol. Bottom trace represents the 50 pA current step used to evoke the subthreshold depolarization. **B)** Quantification of the average overshoot amplitude presented as a function of peak amplitude, before (black) and after (red) wash-in with 5 µM propofol. A significant decrease in the overshoot amplitude can be observed (n=16, p= 0,00856)

lower. In the propofol example trace, the membrane potential does not overshoot, but instead slowly increases until the end of the current step.

The average overshoot values have been quantified in figure 3.5B. 1 second, 50 pA depolarizing currents were injected and overshoot size was quantified as described in 2.5.5. Results are presented as a function of peak amplitude as the M-channel activity, and thus overshoot size, will depend on input resistance and the size of the depolarization. The overshoot value before wash-in with propofol was 1,083±0,2151 mV, while the overshoot value after wash-in was -0,1518±0,3506 mV (n=16). The two groups have slightly different peak values (baseline: 6,079 mV±0,3788 mV, propofol: 6,226±0,3954 mV. Since the difference in peak amplitude is so small (0,1466 mV difference between means), an assumption that this difference in peak is negligible was made to perform a pair-sample t-test.

One cell did not complete the necessary protocol, and one cell was excluded due to firing of an AP.

Even though the M-channel suppresses subthreshold depolarizations and reduces the probability for reaching the threshold for firing an AP, M-channels also play an important role in the regulation of firing during bursts. If propofol had any effect on M-channel activity, the burst firing pattern should be affected. To investigate this, interspike intervals (the time between two APs) (ISIs) have been examined in figure 3.6. Example traces of 250 ms depolarizations are shown in 3.6A (top). Both traces contain eight spikes and were chosen as an example for the temporal correlation between the first spikes and the last spikes. The two traces are superimposed in figure 3.6B, where the membrane potential is shown on top and the injected current is shown on the bottom. A clear difference in the spiking pattern can be observed between the two traces. During baseline, the first few spikes fired with short ISIs which then gradually increased along the depolarization. After addition of 5 µM propofol, the ISIs were much more uniform along the depolarization. Since the largest difference is at the beginning of the burst, the four first ISIs have been more closely examined in figure 3.6C. These results are averages from all 18 cells. As expected from the example traces, the largest difference occurred at the first ISI (time between the first and second AP), with the difference decreasing gradually. The first three ISI were significantly longer after wash-in, while the duration of the fourth ISI was near identical (baseline: 31,39±0,4032 ms, propofol: 31,45±0,3961 ms). An increase in the duration of the first ISI after application of propofol was seen in 17 out of 18 cells. To test whether this change is a direct result from wash-in of propofol, the duration of the first ISI has been plotted as a function of time in figure 3.6D. As seen in figure 3.6C, there is a clear increase in the duration of the first ISI in the burst. This increase does *not* seem to correlate with the wash-in of propofol, as the measured duration of the first ISI seems to increase linearly the first 30 minutes. No evident change in the rate of the increase can be seen at, or soon after, the wash-in.

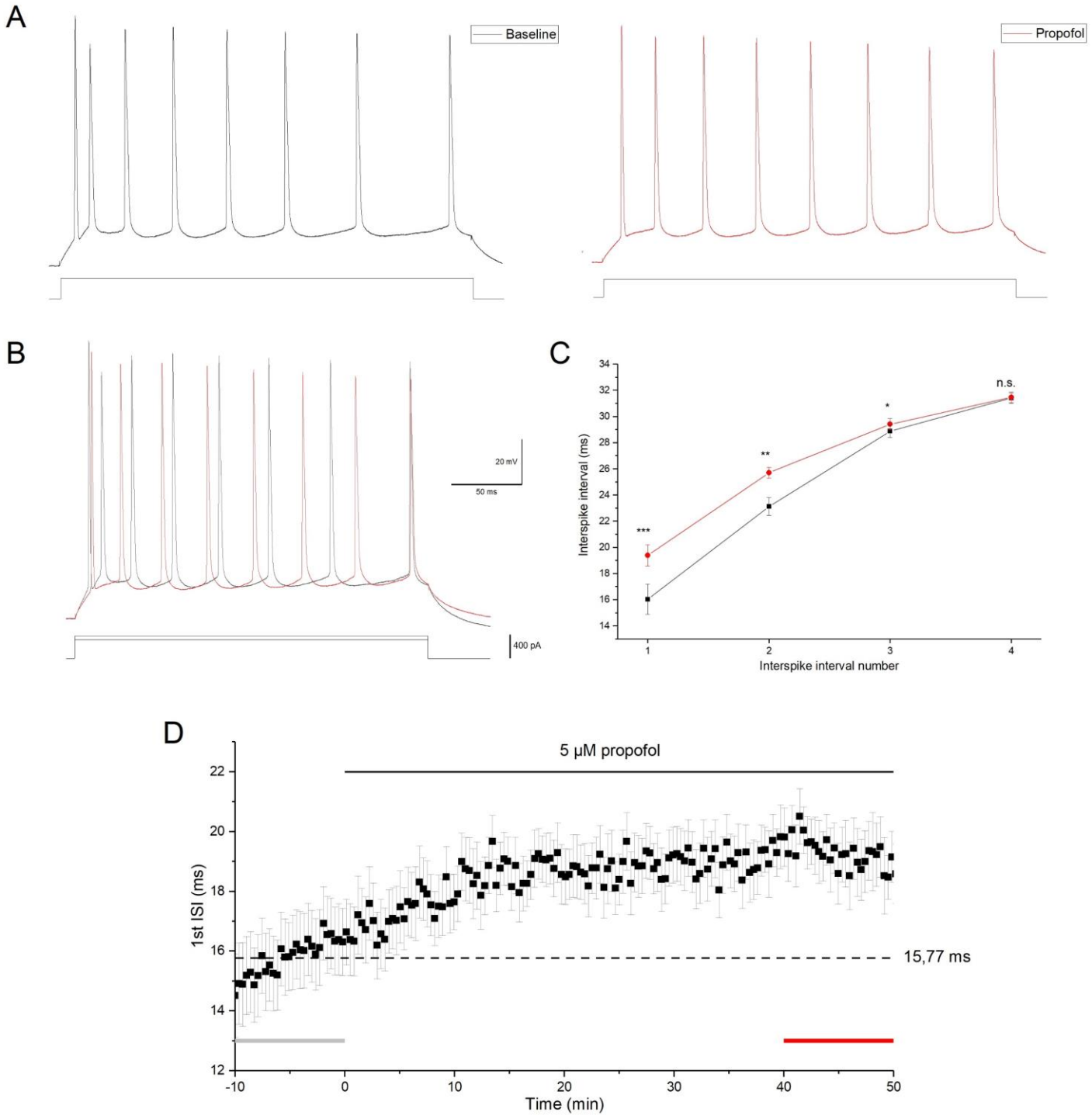

Figure 3.6: Interspike interval. **A)** Example traces from the same cell before (black, left) and after wash-in with 5 µM propofol (red, right), with the injected current pulse below. **B)** Baseline and 5 µM propofol traces superimposed. **C)** Quantification of the first four interspike intervals. The baseline values are averages from the first 10 minutes of a time course, while the "propofol" values are from the last 10 minutes of the time course. A significant increase can be observed for the first 3 intervals, while the fourth interval seems unaffected (n=18, 1st interval; $p=1{,}17522\times10^{-5}$, 2nd interval; $p=8{,}15449\times10^{-5}$, 3rd interval; p=0,1808, 4th interval; p=0,81865). **D)** Time course of the average time between the first and the second spike in the burst (n=18). The dotted line represents the average time during baseline recording. Grey and red bars represent the time intervals used for the analysis in figure C.

3.3 Synaptic transmission

3.3.1 EPSP size

Many anesthetics are known to modulate synaptic transmission, where the majority either enhances GABAergic transmission or inhibits glutamatergic transmission (or both) (Buggy, Nicol, Rowbotham, & Lambert, 2000). To test the effect of propofol on synaptic transmission between the perforant path and CA1 pyramidal cells, perforant path fibers in the SLM were stimulated with five pulses at 50 Hz. To study the effects on glutamatergic transmission and GABAergic transmission separately, the experiments were performed either in the presence of $GABA_A$ receptor antagonist gabazine (+gabazine, n=11) or in the absence of gabazine (-

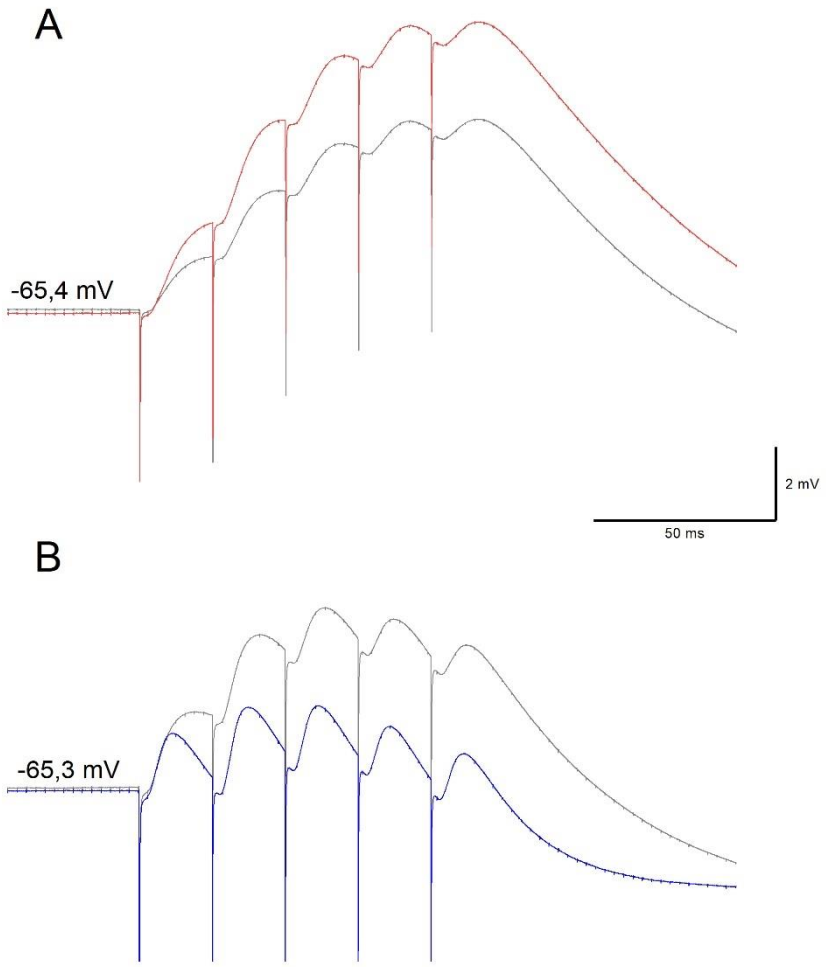

Figure 3.7: Effect of propofol on synaptic transmission. **A)** Average trace of postsynaptic potentials evoked by 50 Hz extracellular SLM stimulation with 5 µM gabazine in the bath (n=11). Red line represents the average postsynaptic potentials in the presence of 5 µM propofol, while the grey line is the average baseline. **B)** Average trace of postsynaptic potentials evoked by 50 Hz extracellular SLM stimulation in absence of the $GABA_A$-blocker gabazine (n=7). Grey line represents the average baseline EPSPs, while the blue trace represents the EPSP after application of propofol.

gabazine, n=7). The evoked postsynaptic potentials in CA1 pyramidal cells were recorded and are shown in figure 3.7. Figure 3.7A shows the average postsynaptic response in the presence of 5 µM gabazine. Any traces where an AP was evoked have been excluded. After application of 5 µM propofol, a clear increase in all five EPSPs can be observed. Figure 3.7B illustrates the average postsynaptic response in absence of gabazine. A decrease in all EPSP can be observed. This is expected, as studies have shown a potentiating effect of propofol on $GABA_A$ receptors (Adodra & Hales, 1995; Hales & Lambert, 1991).

3.3.2 Temporal summation

Changes in the properties of postsynaptic summation of EPSPs can largely affect the output of a cell, and affect the impact of different inputs on a cell's firing. Both HCN channels and M-channels, two of the channels involved in mAHP, have been shown to inhibit temporal summation in CA1 pyramidal cells. To investigate if the changes in the peak amplitude of the fifth EPSP are a result of changes in temporal summation, the peak of the fifth EPSPs have been compared to the peak of the first EPSP in figure 3.8.

Figure 3.8A compares the changes in the peak of the first and fifth EPSP in +gabazine (top) and in -gabazine (bottom) in response to the application of 5 µM propofol. In +gabazine (top), the amplitude of both the first and fifth EPSP seem to increase after wash-in of propofol. A close to proportional change can be observed between the first and fifth EPSP. In -gabazine (bottom), the first EPSP did not seem to be affected by propofol wash-in as no clear change in amplitude can be seen around time = 0 min. The fifth EPSP in -gabazine seems to decrease as a result of propofol wash-in. The amplitudes of both peaks in both groups before and after application of propofol have been quantified and compared in figure 3.8B. Both the fifth EPSP and the first EPSP increased significantly in +gabazine, where the first EPSP increased from 1,616±0,2098 mV at baseline to 2,622±0,3608 mV after application of propofol. The fifth peak increased from 5,500±0,5759 mV to 8,217±1,012 mV after application of propofol, corresponding to a 49,4% increase. This increase was observed in 8 out of 11 cells. In -gabazine, no significant change was observed at the peak of the first where the peak decreased from 2,280±0,5017 mV to 1,833±0,5332 mV after application of propofol. The fifth peak decreased significantly from 4,072±0,8759 mV to 1,182±1,034 mV after propofol

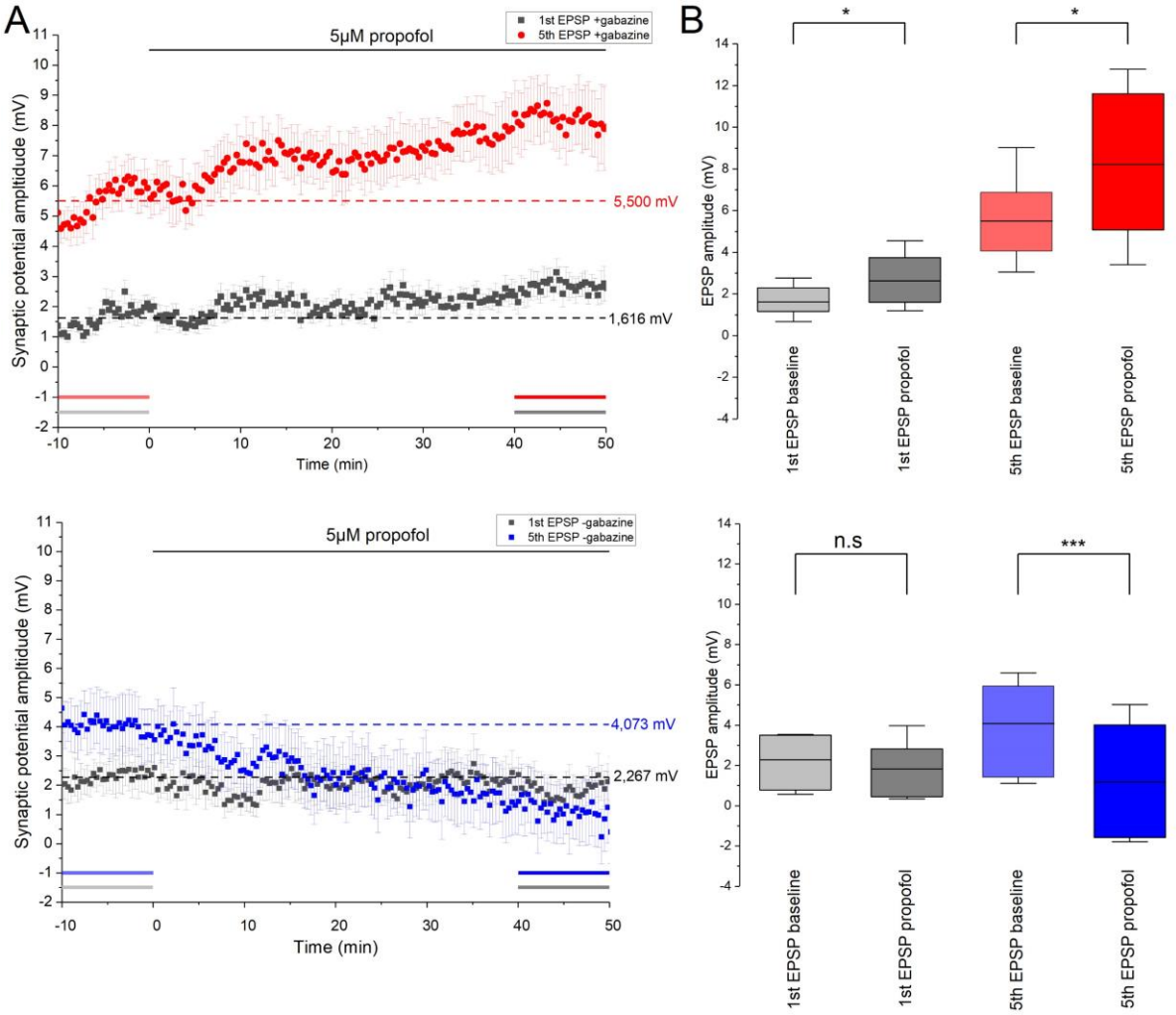

Figure 3.8: Effect of propofol on temporal summation from perforant path stimulation. **A)** Time course of the peak amplitudes of the first and fifth EPSP in +gabazine (top) and in -gabazine (bottom). Dotted lines with the related number indicate the average peak amplitude during baseline. Grey, red, and blue bars represent the time interval used for quantification in figure B. **B)** Quantification of the peak amplitude of the and the first and the fifth EPSP before and after wash-in with 5 µM propofol. Top graph (grey and red) shows the peak amplitudes in +gabazine, while bottom graph (grey and blue) shows the peak amplitudes in -gabazine. Top: A significant increase can be observed in both the peak of the first and the fifth EPSP after application of 5 µM propofol (1^{st}: p= 0,02963, 5^{th}: 0,02029, n=11). Bottom: No significant change in the peak of the first EPSP, but the peak of the 5^{th} decreased significantly after application of propofol (1^{st}: p=0,06131, 5^{th}: p=5,23279×10^{-4}, n=7).

wash-in. The mean peak amplitude of the fifth EPSP decreased by 71,96%. A decrease in the peak amplitude of the fifth EPSP was observed in all 7 cells tested without gabazine.

To investigate the role of these observed changes in temporal summation, ratios between the fifth EPSP and the first EPSP have been plotted in figure 3.9. In figure 3.9A, the fifth/first ratio is plotted for +gabazine for before and after application of propofol. No significant change can be observed. This indicates that the observed increase in EPSP amplitude observed in figure 3.7A is *not* a result of increased temporal summation, but rather an

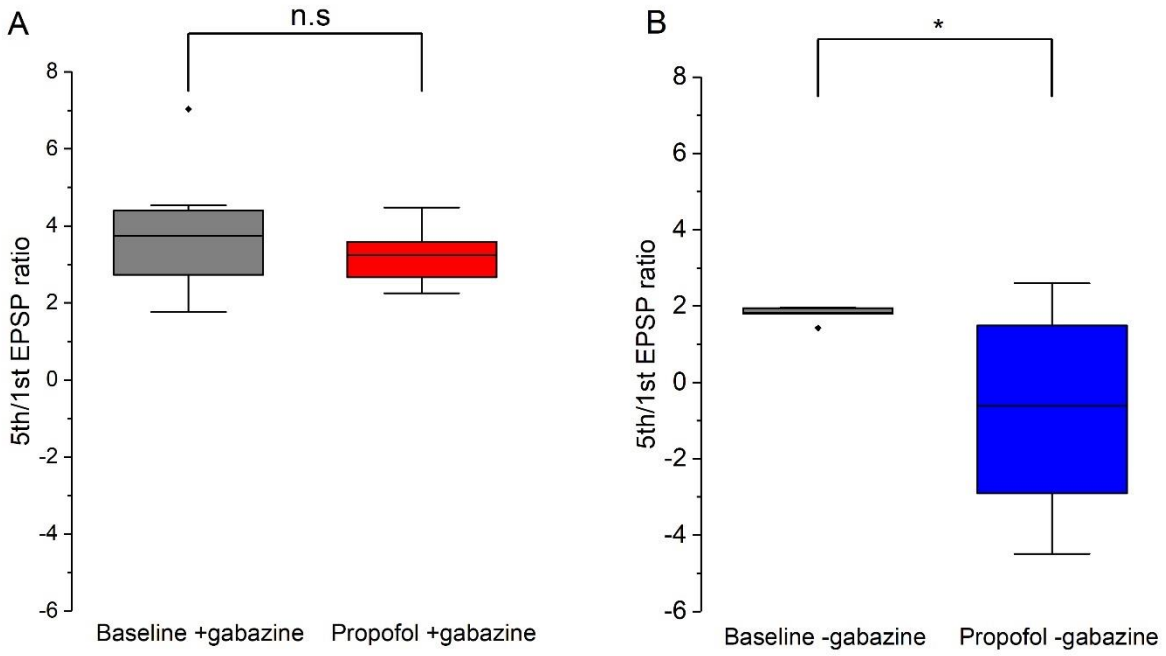

Figure 3.9: Ratio between the peak amplitude of the first and of the fifth EPSP. **A)** No significant change in the fifth/first EPSP ratio can be observed in +gabazine after application of 5 µM propofol (p= 0,25088, n=11). **B)** A significant decrease can be observed in the fifth/first ratio in -gabazine (p=0,0494, n=7).

amplification of every EPSP. Figure 3.9B shows the fifth/first ratio for -gabazine cells, and a clear and significant decrease can be seen for the ratio after application of propofol. This suggests that propofol reduced the amplitude of the 5th EPSP by reducing temporal summation. This corresponds well with figure 3.7B, where a faster decay of every EPSP is observed after propofol, which decreases the window for temporal summation.

3.3.3 Presynaptic modulation

Synaptic transmission involves a presynaptic terminal and a postsynaptic terminal, where both sides of the synapse can be modulated. One frequently used method to investigate a possible presynaptic change is through paired pulses. A change in the paired pulse ratio can often indicate a change in presynaptic short-term plasticity, as mentioned in 2.5.4. Average traces are shown in figure 3.10A, with +gabazine cells top (red) and -gabazine cells bottom (blue). Time courses of both groups are plotted out in 3.10B. There is no clear change in the paired pulse ratio to in response to the application of propofol. The paired pulse ratio before and after application of propofol have been quantified in 3.10C. No significant change was observed in either +gabazine (baseline: 0,9190±0,1926, propofol: 1,184±0,08189, p= 0,17039, n=11) or in the -gabazine group (baseline: 1,169±0,08688, propofol: 1,050±0,1023, p= 0,40239, n=7).

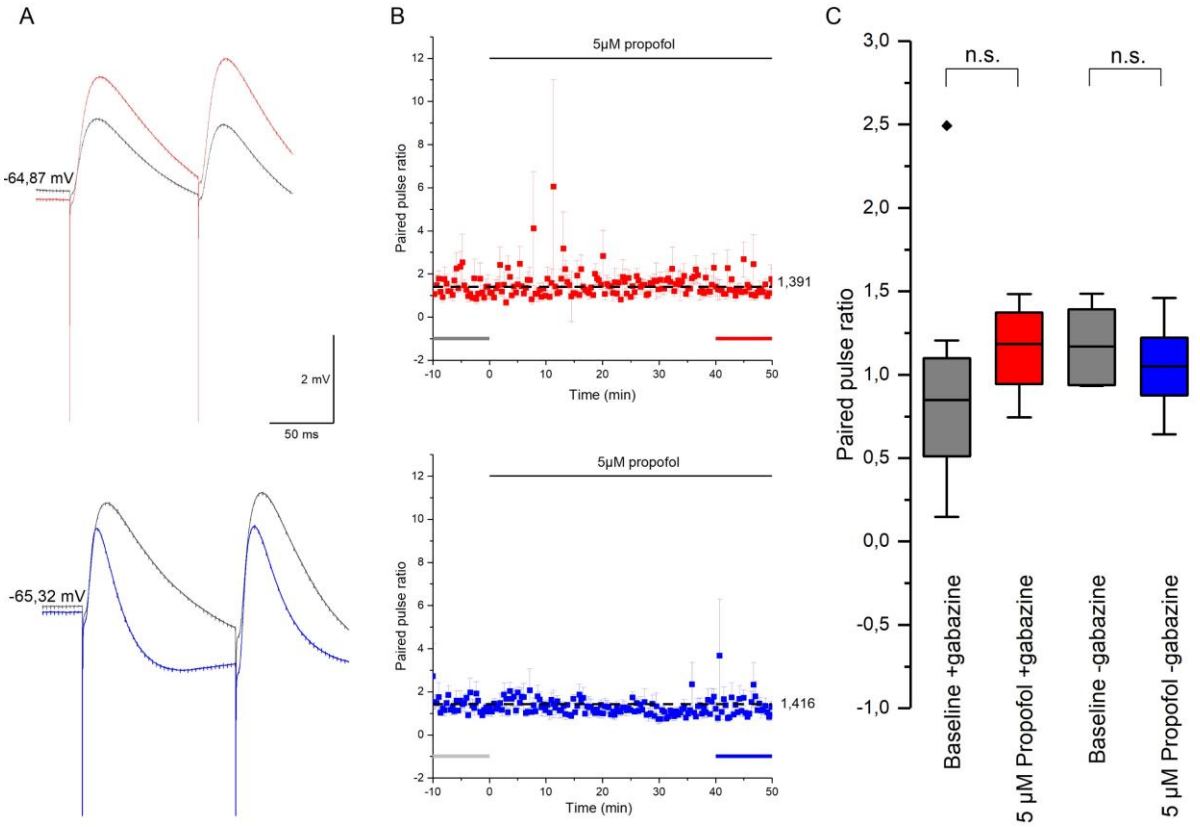

Figure 3.10: Effect of propofol on paired pulse facilitation. **A)** Average traces from the paired pulses in the presence of gabazine (top) and in the absence of gabazine (bottom). No obvious change in the ratio between these. **B)** Time course of the paired pulse, shown as the rise slope of the second pulse divided by the rise slope of the first pulse. Top graph shows +gabazine (red), while bottom graph shows -gabazine (blue). Grey, red, and blue bars represent the time interval analyzed in figure C. **C)** Quantification of paired pulse ratio. No significant change in either groups (+gabazine; p= 0,17039, n=11, -gabazine; p= 0,40239, n=7)

4 Discussion

These results indicate that propofol can affect afterhyperpolarization in CA1 pyramidal cells, where both sAHP and mAHP decreased is the size. Despite observing these effects in most of the cells tested, the credibility of some of these findings has to be questioned. Both in the sAHP and mAHP time courses, the size decreased slowly during baseline. After application of 5 µM propofol, an increase in the rate of change of mAHP can be observed. A clear change in the rate of decrease in sAHP size was not observed after application of propofol. These results and possible explanations will be further discussed in 4.2.1 and 4.2.2.

The synaptic potential from perforant path stimulation indicates that propofol both increases EPSP and IPSPs. The inhibitory effect of propofol is well-known and results from the potentiation of $GABA_A$ receptors (Bai, Pennefather, MacDonald, & Orser, 1999). This inhibitory effect was seen in all 7 CA1 pyramidal cells tested without gabazine. An amplification of EPSP by propofol has, to the best of my knowledge, not been reported before and will be further discussed in 4.3.1.

Even though some of the results were significant, and clear changes could be observed, some factors have to be taken into consideration when interpreting these results.

Due to different difficulties and changes during the course of the project, there was too little time left to perform control experiments. Ideally, these would have been performed under the same circumstances as the experimental groups and using an emulsion containing all the components except propofol.

The stability and quality of the acquired results are variable. Due to low sample number and short time, several cells that would under different circumstances be excluded were included. One of the main issues with the results acquired from several of the cells is the appearance of a low-frequency oscillation which affected several of the studied parameters, including input resistance, EPSP amplitude, and AHP size. This oscillation occurred most often with a frequency of about one wave per 10th minute and was observed in eight out of the 18 cells used in these experiments. This resulted in an unstable baseline and increased the difficulty of interpreting the results.

In discussing the results, time courses will be emphasized. The reason behind this is that time courses give a more credible representation of the change. This is especially important in this case, as the before and after data points might be from different phases of the slow oscillations observed. Not all parameters could be or were observed during the time course, and will only be presented with a before and after graph.

4.1 Methodological issues

Whole-cell patch clamp is an invasive technique, and will to some extent affect the cells electrical properties over time. The neuronal cell body contains many important intracellular factors, which are necessary for normal function or modulation of channel function. The intracellular pipette solution is a simplified version of the actual intracellular solution, having a similar ionic composition and pH-value, but lacking many of the factors found in the cytosol of a cell. A prolonged whole-cell recording may result in some of these factors diffusing into the pipette, consequently diluting the factor(s) in the cell body. Each cell was tested for over an hour, which could have affected the studied parameters.

In addition to the dilution of intracellular factors, there is also a lack of extracellular factors. As mentioned in 1.2.3, the sAHP is highly modifiable and is influenced by several factors in vivo, such as acetylcholine and noradrenaline. The lack of these different factors could potentially result in different effects on sAHP by propofol *in vivo* and *in vitro*. This will be further discussed in 4.2.2.

One of the limitations of patch-clamp is the temperature. Due to the limited oxygen supply to the cells, the bath temperature had to be lower than the physiological temperature to reduce the metabolism of the neuronal cells in the slice and increase the survivability. Even though the temperature difference between 37°C and 31°C is not large, the kinetics of different intrinsic properties could be affected. In fact, sAHP have been shown to exhibit some temperature-dependence where the sAHP amplitude and duration is increased at 32°C relative to 37°C. (S. M. Thompson, Masukawa, & Prince, 1985). Whether this could affect the effect of propofol on the studied parameters is unknown.

4.1.1 Propofol issues

Due to the lack of control experiments, effects caused by the solvents in the emulsion cannot be excluded. Though the different components of the emulsion were likely chosen due to their lack of effect on the central nervous system, some of these components might not cross the blood-brain barrier *in vivo* to have an effect. By direct application of the emulsion onto a brain slice, these components could potentially affect neuronal properties.

Propofol was diluted to 5 µM in aCSF, but the actual concentration reaching the recording chamber is unknown. A study from 2017 showed that propofol in gaseous form largely adhered to silicone tubing, like the ones used in these experiments, and that only ~10% reached the end of a one-meter long tube (Maurer et al., 2017). Though these kinetics most likely differ for gaseous and aqueous propofol (as used in this thesis), some adherence to the tubing is to be expected.

4.2 Effect on afterhyperpolarization

4.2.1 Slow afterhyperpolarization

Though sAHP size seemed to decrease after wash-in with propofol, contrary to the hypothesis, the credibility of these effects has to be questioned.

Firstly, there is no clear change in the rate of decrease in sAHP size at or around the time of propofol wash-in in figure 3.2A. This could partially be “masked” by an increase in input resistance, where the application of propofol leads to a decrease in sAHP size, but the increased input resistance increases the size simultaneously. Though theoretically possible, it is unlikely as no clear correlation between wash-in of propofol and change in sAHP was seen in any cells, even in cases where there was close to no change in input resistance.

And secondly, a decrease in sAHP over time during patch-clamp recordings has also been reported. Paola Pedarzani, Krause, Haug, Storm, and Stühmer (1998) showed an initial increase in sAHP size and duration the first minutes after establishing the whole-cell configuration, which then gradually decreased by 12.6 ±2,5% after an hour. This initial increase in sAHP size would then occur before the time course experiment, as the time course was usually initiated 10-30 minutes after establishing whole-cell configuration. This time-

dependent decrease in sAHP could contribute to the observed results in this thesis. One of the explanations behind this decrease is the dilution of intracellular factors. The intracellular calcium sensor hippocalcin has been linked to sAHP, where a hippocalcin knock-out had significantly smaller sAHP (Kim, Kobayashi, Takamatsu, & Tzingounis, 2012; Tzingounis et al., 2007). Since hippocalcin is a relatively small and soluble protein (Helassa, Antonyuk, Lian, Haynes, & Burgoyne, 2017; Tzingounis et al., 2007), it could potentially diffuse into the pipette solution, effectively reducing the intracellular hippocalcin concentration in the cell body.

A reason why the experiments did not yield the expected results, could be due to the lack of acetylcholine or other neuromodulators in the aCSF. We hypothesized that in wakefulness, the sAHP in cortical neurons is small due to the actions of several neuromodulators such as acetylcholine and noradrenaline. When transitioning into deep sleep, the sAHP is theorized to increase in size. The same is hypothesized to be true for general anesthesia. A possible mechanism for increasing the sAHP size is through inhibition of neuromodulatory action, rather than directly affecting sAHP. This way, propofol could increase sAHP size *in vivo*, but fail to do the same *in vitro*. By inhibiting either the signal transduction or the binding of ACh to the receptor, the inhibitory function of ACh on sAHP could be blocked. In fact, studies have shown that propofol binds to muscarinic receptor M_1, and attenuates M_1-mediated signal transduction in oocytes expressing rat M_1-receptors (Murasaki et al., 2003; Nagase et al., 1999).

4.2.2 Medium afterhyperpolarization

Application of propofol seemed to decrease the peak of mAHP in CA1 pyramidal cells. Though all cells showed a decrease in mAHP peak amplitude, only a few cells displayed a clear direct response to the application of propofol. This is possibly due to some oscillatory noise observed in the results, but could also be that propofol has no direct effects on the mAHP.

The time course (figure 3.3A), which is an average of the time courses from 16 cells, shows a decrease in mAHP which seems to be correlated with the time of propofol wash-in. Since the underlying channels behind mAHP in CA1 pyramidal cells are mostly known, different intrinsic properties were analyzed to test for the activity of HCN channels and M-channels, two of the channels known to mediate the mAHP.

HCN channels

HCN channels are activated by hyperpolarization, and HCN channel activity is often characterized by the sag in negative current steps. In these experiments, there was no evidence of any change in the sag in any of the protocols following the application of propofol. There was a small shift between the two regression lines, but this could be due to high intra-sample variability. Furthermore, inhibition of HCN channels would not shift the line, but change the slope of the regression line relative to the baseline regression line. Both baseline and propofol regression lines should produce a 0 mV large sag when the peak is 0 mV. Inhibition of HCN channels should result in a less steep slope, as a smaller sag would be produced as a response to the same hyperpolarization. There is no obvious difference in the slope between the two regression lines.

As mentioned in 1.2.5, HCN channel activity is important for the integration of synaptic potentials. As the concentration of HCN channels increases with distance from the soma (Kole, Hallermann, & Stuart, 2006; Lörincz, Notomi, Tamás, Shigemoto, & Nusser, 2002), a large effect should be observed on distal input (as the ones used in these experiments) if the HCN channels were inhibited (Magee, 1999). An inhibition of HCN channels should increase temporal summation, which is not observed in +gabazine.

The change in mAHP was significant at all membrane potentials tested (-70 mV to -55 mV, 5 mV increments). Gu et al. (2005) showed that blocking HCN channels with the selective blocker ZD7288 at an RMP of -60 mV, did not affect mAHP size. But when the RMP was held at -80 mV and ZD7288 was applied, a significant decrease in mAHP size was observed. So in addition to not seeing any change in HCN channel activity, inhibition of HCN channels would not explain the significant change in mAHP peak observed at RMPs of -60 mV and -55 mV.

These results are as expected, as high concentrations of propofol are reported to be needed to affect HCN channel activity in CA1 pyramidal cells. Funahashi et al. (2004) showed that a concentration of 235 μM propofol is needed to inhibit the HCN-current by 50% in CA1 pyramidal cells. A similar value was also found by Higuchi et al. (2003).

M-channels

According to Gu et al. (2005), mAHP in CA1 are only controlled by HCN channels and M-channels, and that HCN channels are the main contributors at RMPs negative to -72 mV while M-channels are the main contributors at RMPs positive to -72 mV. The most negative RMP used in these experiments was -70 mV, and thus any observed mAHP should be mainly due to M-channels.

Two different intrinsic properties were investigated in order to examine a possible effect on M-channels. Firstly, the overshoot amplitude during subthreshold positive current steps was investigated. The overshoot amplitude seemed to decrease after application, suggesting a reduced inhibition of subthreshold potentials. This decrease in overshoot amplitude is not unique for inhibition of M-channel, and the same effect is illustrated by blockage of HCN channels by Robinson and Siegelbaum (2003). As no change was observed in HCN channel activity, these results point to an inhibition of M-channels. Though this does not confirm it, a decreased overshoot is an expected outcome of M-channel inhibition in CA1 pyramidal cells.

The second parameter investigated were the ISIs. The change in the pattern observed in these results is similar to the results Gu et al. (2005) produced by blocking M-channel activity both experimentally and *in silico* at a holding potential of -60 mV. But from figure 3.6D, no correlation between the wash-in of propofol and the change in the duration of the first ISI can be observed. This could be due to no actual effect of propofol on the first ISI, or due to the low quality of the cells. Both of the two properties investigated point to a change in a decreased M-channel activity, though there is no direct evidence of propofol inducing this change.

After application of propofol, a change in the relationship between the size of the injected current and mAHP could be observed in figure 3.3C (right). During the baseline recording, a close to a linear relationship could be observed, while after application there was no increase of mAHP peak amplitude from 0 pA to 150 pA. Since M-channels are voltage-gated, mAHPs can be produced even from subthreshold depolarizations. If these were to be blocked, then SK channel can partially "take over". Studies have shown that SK channels do not contribute to mAHP in CA1 pyramidal cells, *unless* M-channels are inhibited (S. Chen et al., 2014; Gu et al., 2008). This would explain why there was no observable difference in current injections from 0 pA to 150 pA, where spiking frequency and the accumulated intracellular Ca^{2+}

concentration is low. In these ranges, M-channels would be open due to their voltage-gating. With increasing current amplitude, the spiking frequency increases along with intracellular Ca^{2+} concentration, and potentially result in progressively larger mAHP caused by the SK channel. These observations could also be explained by an increased voltage-dependency, where binding of propofol resulted in M-channel requiring a stronger depolarization to open.

Another possibility could have been that the depolarizations after the application of propofol were lower than during baseline recordings or that the AP frequency was reduced. This was not the case, as the input resistance increased (appendix 5.1, figure 5.1), increasing the size of the depolarizations. Additionally, the AP frequency at all current steps (50 pA -400 pA) increased after application of propofol (data not shown).

In figure 3.3C (left), a decreased mAHP amplitude can be observed at all RMPs tested. Even though M-channels are reported to be the main contributors to mAHP at all these resting potentials, a larger difference between the baseline and after application of propofol should be observed at -55 mV than at -70 mV. This is due to the driving force (the equilibrium potential – the membrane potential) for K^+. When the membrane potential is held at a depolarized potential (-55 mV), the driving force for K^+ is large. At more hyperpolarized potentials (-70 mV), the membrane potential is closer to the equilibrium potential of K^+, and therefore the driving force is smaller. These differences in driving force between the two RMPs mean that K^+ should have a larger tendency to diffuse into the cell at -55 mV than at -70 mV, and that a larger fraction of the mAHP at -55 mV than at -70 mV is due to M-channel conductance. An inhibition of M-channels at -55 mV should therefore have a larger impact on mAHP than an inhibition of M-channels at -70 mV. This trend was not seen in figure 3.3C (left), where a larger change can be observed at -70 mV than at -55 mV, suggesting that the observed change in mAHP might not be due to M-channel inhibition, or due to inhibition of M-channel along with another channel affecting mAHP at more hyperpolarized RMPs. The only other (known) channel to affect the mAHP in CA1 pyramidal cells at more hyperpolarized RMPs is the HCN channel, but as mentioned above, no change in HCN channel activity was observed.

SK channels

A possible inhibition of SK channels by propofol is not unlikely. In fact, propofol has been shown to block SK channel in thalamic GABAergic neurons using a 3 µM concentration (Ying & Goldstein, 2005a). In these experiments, CA1 pyramidal cells also showed a

significant decrease in mAHP after application of propofol. Whether propofol affects SK channels in CA1 pyramidal with similar concentrations is unknown.

SK channels are in similarity with M-channels, permeable to K^+. The same issue occurs when trying to explain the voltage-dependence of the changes observed in mAHP. The decrease in mAHP amplitude seems larger at the more hyperpolarized potentials (-70 mV and -65 mV) than at the more depolarized potentials (-60 mV and -55 mV). An inhibition of SK channels should affect the mAHP at -55 mV to a greater extent than at -70 mV.

As mentioned in 1.2.4, the contribution of these channels to the mAHP in CA1 pyramidal is not completely agreed upon, and some studies have shown that the SK channel only contributes to the mAHP when M-channels are non-functional (Gu et al., 2008). This would mean that the observed effect on mAHP cannot be due to inhibition of SK channels unless propofol also blocks M-channels. To confirm or deny this, further studies are required. For suggestions for future studies to determine which of these channels are affected, see 4.4.

4.3 Effect on synaptic transmission

After wash-in with propofol, the EPSP size seemed to increase. Due to some oscillatory noise, it is difficult to determine if the observed increase in EPSP size is directly correlated with the wash-in with propofol. This increase seemed to be proportional between the first and the last EPSP in the train, indicating that the observed effects were not due to an increased temporal summation but rather to an amplification of EPSPs in general. An increased summation would be expected if either HCN channels or M-channels were inhibited. The role of M-channels in temporal summation has been shown to depend on the location in the dorsoventral axis of the hippocampus, where M-channels inhibit summation to a larger degree in dorsal cells (Hönigsperger, Marosi, Murphy, & Storm, 2015). As the location in the laterodorsal axis was not taken into account, the exact expected effect of inhibition of M-channels is unknown.

Another possibility is through LTP, where the synaptic strength is enhanced. The insertion of new AMPA receptors or enhancement of their conductance could explain the proportional increase in EPSPs, and could also explain the lack of an obvious baseline and plateau phase. Though to the best of my knowledge, there have been no reports of 250 ms, 50 Hz stimulation of the perforant path to induce LTP in perforant path-CA1 synapses. But since no NMDA receptor blocker has been used in this thesis, LTP cannot be excluded.

To investigate the observed increase in EPSP could be due to a presynaptic change, the paired pulse ratio was calculated. There was no significant change in the paired pulse ratio in either group (+gabazine, -gabazine) (figure 3.10). Though this does not completely exclude the possibility, it indicates that there were no presynaptic changes.

As mentioned in 4.2, a study has shown that propofol had blocked SK channels in thalamic interneurons at relevant concentrations. Ying and Goldstein (2005a) also showed that propofol-mediated inhibition of SK channels in thalamic interneurons resulted in increased temporal summation of EPSPs. Inhibition of SK channels in CA1 pyramidal cells by application of apamin has been shown to increase the amplitude of a single EPSP (Jones, To, & Stuart, 2017). The fact that the observed increase in EPSP amplitude in these experiments seemed to be amplifications of every single EPSP and not an increase in temporal summation (figure 3.9), correlates well with the observations of Jones et al. (2017). One study showed the effects of inhibition of SK channels in CA1 pyramidal cells by apamin on a 100 Hz postsynaptic potentials (Ngo-Anh et al., 2005), where the observed change is similar to those in figure 3.7A. Ngo-Anh et al. (2005) did not quantify the summation in these postsynaptic potentials, but an increase in the amplitude of both the first and the fifth EPSP can be observed. Ngo-Anh et al. (2005) did not observe any significant change in the paired pulse ratio. The similar effects on EPSPs observed by inhibition SK channels and application of propofol strengthens the theory that the observed increase in EPSP size observed in figure 3.7A is a result of propofol-mediated inhibition of SK channels.

An effect on GABAergic transmission by propofol has been known for a long time. A study has also shown that propofol inhibited temporal summation in thalamic relay neurons by potentiation of $GABA_A$ receptors (Ying & Goldstein, 2005b). These results are similar to the acquired results from the CA1 pyramidal cells, where a decrease in summation was observed in -gabazine, but no decrease in +gabazine. This shows the strong potentiating effect of propofol on $GABA_A$-receptors. Since an amplification of EPSP size was observed in +gabazine, this effect had to be counteracted and overwhelmed by the effects of propofol on the $GABA_A$ receptor. Since the effect on $GABA_A$ receptors by propofol is well known and strong effect inhibitory effect on the last EPSP was observed in -gabazine but not in +gabazine, I can say with high certainty that propofol did reach the recording chamber and had an effect on the CA1 pyramidal cells.

4.4 Future research

As the results were inconclusive, the experiments could be repeated with some improvements. Firstly, control experiments are needed to exclude the possibility that the observed effects are artifacts. This implies acquiring pure propofol and dissolving it in either dimethyl sulfoxide (DMSO), ethanol, or Intralipid® (emulsion containing soybean oil, glycerin, and phospholipids). In the control experiment only the solvent, without propofol, would be used.

To be able to quantify and measure the afterhyperpolarization more precisely, separate experiments could be set up in which one of the afterhyperpolarizations were blocked. To study the sAHP, an mAHP-blocker could have been added. The M-channel blocker XE-991 has been shown to block I_{mAHP} at subthreshold resting potentials, and only affects sAHP indirectly through an increase in input resistance (Gu et al., 2005). Gu et al. (2005) also used forskolin, an adenylyl cyclase activator, to inhibit the sAHP. Performing separate experiments for sAHP and mAHP, with forskolin and XE-991 respectively, could give a more accurate representation of the effect of propofol.

The increase in EPSP amplitude could be a result of LTP. To reduce this possibility, APV, an NMDAR-blocker, could be added to prevent NMDAR-dependent LTP. Control experiments would still be necessary to exclude any non-LTP-related changes in synaptic potential amplitude, which could arise from drift of either the stimulation pipette or of the slice relative to each other, or arise from time-dependent changes as a result of the whole-cell configuration, or any other propofol-independent effects.

As mentioned in 4.2.2, one of the reasons why sAHP did not decrease in response to propofol, could be because propofol modulates sAHP indirectly. Acetylcholine, which is normally abundant at wakefulness, reduces the sAHP size. By blocking the effects of ACh, the sAHP could increase. To test this hypothesis, an experiment with ACh, or with the more stable cholinergic agonist carbachol, could be set up. In this experiment, the slice would first be exposed to propofol for a period of time, before carbachol is washed in. The control experiment would be carbachol wash-in without the presence of propofol. Under normal condition carbachol abolishes the sAHP, but if propofol blocks or reduces the binding of carbachol to cholinergic receptors, a smaller change in the sAHP would be observed than in the control experiment without propofol. Additionally, specific agonists for different subtypes of muscarinic receptors could be used to identify the mechanisms of action.

To be able to determine the molecular target behind the change in mAHP with higher certainty, specific blockers of the possible targets can be used in combination with propofol to see if propofol has any effect on mAHP when each of the potential channels is specifically blocked, with ZD7288 for HCN channel, XE991 for M-channel, and apamin/Ca^{2+}-free aCSF for SK channel. In these experiments, slices would then be incubated with these blockers before the experiment begins. Additionally, more negative holding potential than -70 mV (-80 mV or -90 mV) could have been tried to better test for HCN channel activity.

It could also be interesting to look at the effect of propofol on EPSPs at different frequencies. As seen in figure 3.7B (-gabazine), the slope of the first EPSP seemed to be unchanged after application of 5 µM propofol, but the EPSPs seemed to decay faster, which can effectively reduce the time window for temporal summation. To investigate further how propofol affects summation, one could try to stimulate perforant path fibers at a higher frequency and observe the effect. Optimally, the frequency would be adjusted so that the next EPSP begins at the peak of the last, and compare these results with higher and lower frequencies. The change in the decay rate of the EPSPs might be dependent on propofol concentration, which could result in different frequencies being favored at different concentrations. The experiments could be done with a small range of assumed physiologically relevant propofol concentrations (0,1 µM, 1,0 µM, and 10 µM), and in the presence of NMDA receptor-blocker APV to prevent any LTP.

Due to our inexperience with propofol and its cellular effects, long time courses were performed and values from the beginning and the end were chosen and compared. In future experiments, this time could be reduced from one hour to 30 or 45 minutes. This could improve the quality of the recordings acquired after the time course, increase productivity, and possibly increase the number of cells surviving for the duration of the recordings.

4.5 Conclusion

As the project was cut short, most of the results are inconclusive and require further studying to confirm. Based on the results acquired, the following can be said about the effect of propofol on CA1 pyramidal cells:

- The sAHP seemed to decrease over the duration of the recording, but whether the decrease was directly correlated with propofol application is yet to be determined.
- Propofol seemed to decrease the amplitude of mAHP, but further studies with higher quality results are required to confirm this.
- HCN channel activity did not seem to be affected by the application of 5 µM propofol.
- Neither HCN-, SK-, nor M-channels were perfect candidates for the change in mAHP, as changes in other intrinsic properties did not match the expected results for inhibition of these channels. Inhibition of M-channels or SK channel or both by propofol seems the most likely mechanism for the observed decrease in mAHP amplitude.
- An increase in EPSP size was observed after application of 5 µM propofol in the absence of inhibitory input. This increase in size did not seem to result from changes in temporal summation, but rather an amplification of each individual EPSP. A likely mechanism for this change is an inhibition of SK channels.
- In the presence of inhibitory input EPSP amplitude decreased after application of propofol. This effect seemed more prominent in late EPSPs rather than in early EPSPs. Additionally, an increase EPSP decay rate was observed, suggesting that the increased inhibition observed after propofol application can be at least partially attributed to decreased temporal summation.

References

Abrams, P., Andersson, K.-E., Buccafusco, J. J., Chapple, C., de Groat, W. C., Fryer, A. D., . . . Wein, A. J. (2006). Muscarinic receptors: their distribution and function in body systems, and the implications for treating overactive bladder. *British Journal of Pharmacology, 148*(5), 565-578. doi:10.1038/sj.bjp.0706780

Adodra, S., & Hales, T. G. (1995). Potentiation, activation and blockade of GABAA receptors of clonal murine hypothalamic GT1-7 neurones by propofol. *British Journal of Pharmacology, 115*(6), 953-960. doi:10.1111/j.1476-5381.1995.tb15903.x

Aeschbach, D., & Borbély, A. A. (1993). All-night dynamics of the human sleep EEG. *Journal of Sleep Research, 2*(2), 70-81. doi:10.1111/j.1365-2869.1993.tb00065.x

Andrade, R., & Nicoll, R. A. (1987). Pharmacologically distinct actions of serotonin on single pyramidal neurones of the rat hippocampus recorded in vitro. *The Journal of Physiology, 394*, 99-124.

Araneda, R., & Andrade, R. (1991). 5-Hydroxytryptamine2 and 5-hydroxytryptamine1A receptors mediate opposing responses on membrane excitability in rat association cortex. *Neuroscience, 40*(2), 399-412. doi:https://doi.org/10.1016/0306-4522(91)90128-B

Avery, M. C., & Krichmar, J. L. (2017). Neuromodulatory Systems and Their Interactions: A Review of Models, Theories, and Experiments. *Frontiers in Neural Circuits, 11*(108). doi:10.3389/fncir.2017.00108

Bai, D., Pennefather, P. S., MacDonald, J. F., & Orser, B. A. (1999). The General Anesthetic Propofol Slows Deactivation and Desensitization of GABA_A Receptors. *The Journal of Neuroscience, 19*(24), 10635. doi:10.1523/JNEUROSCI.19-24-10635.1999

Bear, M. F., & Malenka, R. C. (1994). Synaptic plasticity: LTP and LTD. *Current Opinion in Neurobiology, 4*(3), 389-399. doi:https://doi.org/10.1016/0959-4388(94)90101-5

Bellesi, M., Riedner, B. A., Garcia-Molina, G. N., Cirelli, C., & Tononi, G. (2014). Enhancement of sleep slow waves: underlying mechanisms and practical consequences. *Frontiers in systems neuroscience, 8*, 208-208. doi:10.3389/fnsys.2014.00208

Benardo, L. S., & Prince, D. A. (1982). Cholinergic excitation of mammalian hippocampal pyramidal cells. *Brain Research, 249*(2), 315-331. doi:https://doi.org/10.1016/0006-8993(82)90066-X

Berridge, C. W., Schmeichel, B. E., & España, R. A. (2012). Noradrenergic modulation of wakefulness/arousal. *Sleep medicine reviews, 16*(2), 187-197. doi:10.1016/j.smrv.2011.12.003

Biel, M., Wahl-Schott, C., Michalakis, S., & Zong, X. (2009). Hyperpolarization-Activated Cation Channels: From Genes to Function. *Physiological Reviews, 89*(3), 847-885. doi:10.1152/physrev.00029.2008

Bliss, T. V., & Lomo, T. (1973). Long-lasting potentiation of synaptic transmission in the dentate area of the anaesthetized rabbit following stimulation of the perforant path. *The Journal of Physiology, 232*(2), 331-356.

Bloss, E. B., Cembrowski, M. S., Karsh, B., Colonell, J., Fetter, R. D., & Spruston, N. (2018). Single excitatory axons form clustered synapses onto CA1 pyramidal cell dendrites. *Nature Neuroscience, 21*(3), 353-363. doi:10.1038/s41593-018-0084-6

Bond, C. T., Herson, P. S., Strassmaier, T., Hammond, R., Stackman, R., Maylie, J., & Adelman, J. P. (2004). Small Conductance Ca2+-Activated K+ Channel Knock-Out

Mice Reveal the Identity of Calcium-Dependent Afterhyperpolarization Currents. *The Journal of Neuroscience, 24*(23), 5301. doi:10.1523/JNEUROSCI.0182-04.2004
Brown, D. A., & Passmore, G. M. (2009). Neural KCNQ (Kv7) channels. *British Journal of Pharmacology, 156*(8), 1185-1195. doi:10.1111/j.1476-5381.2009.00111.x
Brown, E. N., Lydic, R., & Schiff, N. D. (2010). General anesthesia, sleep, and coma. *The New England journal of medicine, 363*(27), 2638-2650. doi:10.1056/NEJMra0808281
Buggy, Donal J., M.D., M.Sc., D.M.E., M.R.C.P.I., F.F.A.R.C.S.I., Nicol, B., Ph.D., Rowbotham, David J., M.D., M.R.C.P., F.F.A.R.C.S.I., F.R.C.A., & Lambert, David G., Ph.D. (2000). Effects of Intravenous Anesthetic Agents on Glutamate Release: A Role for GABAAReceptor–Mediated Inhibition. *Anesthesiology: The Journal of the American Society of Anesthesiologists, 92*(4), 1067-1073.
Buzsaki, G., Bickford, R. G., Ponomareff, G., Thal, L. J., Mandel, R., & Gage, F. H. (1988). Nucleus basalis and thalamic control of neocortical activity in the freely moving rat. *The Journal of Neuroscience, 8*(11), 4007. doi:10.1523/JNEUROSCI.08-11-04007.1988
Cai, X., Liang, C. W., Muralidharan, S., Kao, J. P. Y., Tang, C.-M., & Thompson, S. M. (2004). Unique Roles of SK and Kv4.2 Potassium Channels in Dendritic Integration. *Neuron, 44*(2), 351-364. doi:https://doi.org/10.1016/j.neuron.2004.09.026
Camacho-Arroyo, I., Alvarado, R., Manjarrez, J., & Tapia, R. (1991). Microinjections of muscimol and bicuculline into the pontine reticular formation modify the sleep-waking cycle in the rat. *Neuroscience Letters, 129*(1), 95-97. doi:https://doi.org/10.1016/0304-3940(91)90728-C
Cespuglio, R., Gomez, M. E., Faradji, H., & Jouvet, M. (1982). Alterations in the sleep-waking cycle induced by cooling of the locus coeruleus area. *Electroencephalography and Clinical Neurophysiology, 54*(5), 570-578. doi:https://doi.org/10.1016/0013-4694(82)90042-6
Chen, S., Benninger, F., & Yaari, Y. (2014). Role of Small Conductance Ca2+-Activated K+ Channels in Controlling CA1 Pyramidal Cell Excitability. *The Journal of Neuroscience, 34*(24), 8219. doi:10.1523/JNEUROSCI.0936-14.2014
Chen, X., Shu, S., & Bayliss, D. A. (2005). Suppression of Ih Contributes to Propofol-Induced Inhibition of Mouse Cortical Pyramidal Neurons. *Journal of Neurophysiology, 94*(6), 3872-3883. doi:10.1152/jn.00389.2005
Church, T. W., Brown, J. T., & Marrion, N. V. (2019). β3-Adrenergic receptor-dependent modulation of the medium afterhyperpolarization in rat hippocampal CA1 pyramidal neurons. *Journal of Neurophysiology, 121*(3), 773-784. doi:10.1152/jn.00334.2018
Cloues, R. K., & Sather, W. A. (2003). Afterhyperpolarization Regulates Firing Rate in Neurons of the Suprachiasmatic Nucleus. *The Journal of Neuroscience, 23*(5), 1593. doi:10.1523/JNEUROSCI.23-05-01593.2003
Collingridge, G. L., Kehl, S. J., & McLennan, H. (1983). Excitatory amino acids in synaptic transmission in the Schaffer collateral-commissural pathway of the rat hippocampus. *The Journal of Physiology, 334*, 33-46.
Collins, G. G. S., Probett, G. A., Anson, J., & McLaughlin, N. J. (1984). Excitatory and inhibitory effects of noradrenaline on synaptic transmission in the rat olfactory cortex slice. *Brain Research, 294*(2), 211-223. doi:https://doi.org/10.1016/0006-8993(84)91032-1
Compte, A., Sanchez-Vives, M. V., McCormick, D. A., & Wang, X.-J. (2003). Cellular and Network Mechanisms of Slow Oscillatory Activity (<1 Hz) and Wave Propagations in a Cortical Network Model. *Journal of Neurophysiology, 89*(5), 2707-2725. doi:10.1152/jn.00845.2002

Cowan, R. L., & Wilson, C. J. (1994). Spontaneous firing patterns and axonal projections of single corticostriatal neurons in the rat medial agranular cortex. *Journal of Neurophysiology, 71*(1), 17-32. doi:10.1152/jn.1994.71.1.17
Dasari, S., & Gulledge, A. T. (2011). M1 and M4 receptors modulate hippocampal pyramidal neurons. *Journal of Neurophysiology, 105*(2), 779-792. doi:10.1152/jn.00686.2010
Dijk, D.-J. (2009). Regulation and functional correlates of slow wave sleep. *Journal of clinical sleep medicine : JCSM : official publication of the American Academy of Sleep Medicine, 5*(2 Suppl), S6-S15.
Dzirasa, K., Ribeiro, S., Costa, R., Santos, L. M., Lin, S.-C., Grosmark, A., . . . Nicolelis, M. A. L. (2006). Dopaminergic Control of Sleep–Wake States. *The Journal of Neuroscience, 26*(41), 10577. doi:10.1523/JNEUROSCI.1767-06.2006
Engdahl, O., Abrahams, M., Björnsson, A., Vegfors, M., Norlander, B., Ahlner, J., & Eintrei, C. (1998). Cerebrospinal fluid concentrations of propofol during anaesthesia in humans. *British Journal of Anaesthesia, 81*(6), 957-959. doi:https://doi.org/10.1093/bja/81.6.957
Feng, A. Y., Kaye, A. D., Kaye, R. J., Belani, K., & Urman, R. D. (2017). Novel propofol derivatives and implications for anesthesia practice. *Journal of anaesthesiology, clinical pharmacology, 33*(1), 9-15. doi:10.4103/0970-9185.202205
Fioravante, D., & Regehr, W. G. (2011). Short-term forms of presynaptic plasticity. *Current Opinion in Neurobiology, 21*(2), 269-274. doi:10.1016/j.conb.2011.02.003
Franks, N. P., & Lieb, W. R. (1994). Molecular and cellular mechanisms of general anaesthesia. *Nature, 367*(6464), 607-614. doi:10.1038/367607a0
Froemke, R. C., Poo, M.-m., & Dan, Y. (2005). Spike-timing-dependent synaptic plasticity depends on dendritic location. *Nature, 434*(7030), 221-225. doi:10.1038/nature03366
Funahashi, M., Mitoh, Y., & Matsuo, R. (2004). The sensitivity of hyperpolarization-activated cation current (Ih) to propofol in rat area postrema neurons. *Brain Research, 1015*(1), 198-201. doi:https://doi.org/10.1016/j.brainres.2004.04.043
Fuxe, K., Dahlström, A. B., Jonsson, G., Marcellino, D., Guescini, M., Dam, M., . . . Agnati, L. (2010). The discovery of central monoamine neurons gave volume transmission to the wired brain. *Progress in Neurobiology, 90*(2), 82-100. doi:https://doi.org/10.1016/j.pneurobio.2009.10.012
Gamper, N. (2016). Localised intracellular signalling in neurons. *The Journal of Physiology, 594*(1), 7-8. doi:10.1113/JP271357
Greene, R. W., & Frank, M. G. (2010). Slow Wave Activity During Sleep: Functional and Therapeutic Implications. *The Neuroscientist, 16*(6), 618-633. doi:10.1177/1073858410377064
Gu, N., Hu, H., Vervaeke, K., & Storm, J. F. (2008). SK (KCa2) Channels Do Not Control Somatic Excitability in CA1 Pyramidal Neurons But Can Be Activated by Dendritic Excitatory Synapses and Regulate Their Impact. *Journal of Neurophysiology, 100*(5), 2589-2604. doi:10.1152/jn.90433.2008
Gu, N., Vervaeke, K., Hu, H., & Storm, J. F. (2005). Kv7/KCNQ/M and HCN/h, but not KCa2/SK channels, contribute to the somatic medium after-hyperpolarization and excitability control in CA1 hippocampal pyramidal cells. *The Journal of Physiology, 566*(Pt 3), 689-715. doi:10.1113/jphysiol.2005.086835
Haas, H. L., & Konnerth, A. (1983). Histamine and noradrenaline decrease calcium-activated potassium conductance in hippocampal pyramidal cells. *Nature, 302*(5907), 432-434. doi:10.1038/302432a0
Hales, T. G., & Lambert, J. J. (1991). The actions of propofol on inhibitory amino acid receptors of bovine adrenomedullary chromaffin cells and rodent central neurones.

British Journal of Pharmacology, 104(3), 619-628. doi:10.1111/j.1476-5381.1991.tb12479.x

Hara, D. D. S. M., Kai, D. D. S. Y., & Ikemoto, M. D. Y. (1993). Propofol Activates GABAA Receptor-Chloride Ionophore Complex in Dissociated Hippocampal Pyramidal Neurons of the Rat. *Anesthesiology, 79*(4), 781-788.

Helassa, N., Antonyuk, S. V., Lian, L.-Y., Haynes, L. P., & Burgoyne, R. D. (2017). Biophysical and functional characterization of hippocalcin mutants responsible for human dystonia. *Human Molecular Genetics, 26*(13), 2426-2435. doi:10.1093/hmg/ddx133

Higuchi, H., Funahashi, M., Miyawaki, T., Mitoh, Y., Kohjitani, A., Shimada, M., & Matsuo, R. (2003). Suppression of the hyperpolarization-activated inward current contributes to the inhibitory actions of propofol on rat CA1 and CA3 pyramidal neurons. *Neuroscience Research, 45*(4), 459-472. doi:https://doi.org/10.1016/S0168-0102(03)00003-8

Hill, S., & Tononi, G. (2005). Modeling Sleep and Wakefulness in the Thalamocortical System. *Journal of Neurophysiology, 93*(3), 1671-1698. doi:10.1152/jn.00915.2004

Hu, H., Vervaeke, K., & Storm, J. F. (2007). M-Channels (Kv7/KCNQ Channels) That Regulate Synaptic Integration, Excitability, and Spike Pattern of CA1 Pyramidal Cells Are Located in the Perisomatic Region. *The Journal of Neuroscience, 27*(8), 1853. doi:10.1523/JNEUROSCI.4463-06.2007

Huber, R., Felice Ghilardi, M., Massimini, M., & Tononi, G. (2004). Local sleep and learning. *Nature, 430*(6995), 78-81. doi:10.1038/nature02663

Hönigsperger, C., Marosi, M., Murphy, R., & Storm, J. F. (2015). Dorsoventral differences in Kv7/M-current and its impact on resonance, temporal summation and excitability in rat hippocampal pyramidal cells. *The Journal of Physiology, 593*(7), 1551-1580. doi:10.1113/jphysiol.2014.280826

Jones, S. L., To, M.-S., & Stuart, G. J. (2017). Dendritic small conductance calcium-activated potassium channels activated by action potentials suppress EPSPs and gate spike-timing dependent synaptic plasticity. *eLife, 6*, e30333. doi:10.7554/eLife.30333

Kim, Kwang S., Kobayashi, M., Takamatsu, K., & Tzingounis, Anastasios V. (2012). Hippocalcin and KCNQ Channels Contribute to the Kinetics of the Slow Afterhyperpolarization. *Biophysical journal, 103*(12), 2446-2454. doi:https://doi.org/10.1016/j.bpj.2012.11.002

King, B., Rizwan, Arsalan P., Asmara, H., Heath, Norman C., Engbers, Jordan D. T., Dykstra, S., . . . Turner, Ray W. (2015). IKCa Channels Are a Critical Determinant of the Slow AHP in CA1 Pyramidal Neurons. *Cell Reports, 11*(2), 175-182. doi:https://doi.org/10.1016/j.celrep.2015.03.026

Kitamura, A., Marszalec, W., Yeh, J. Z., & Narahashi, T. (2003). Effects of Halothane and Propofol on Excitatory and Inhibitory Synaptic Transmission in Rat Cortical Neurons. *Journal of Pharmacology and Experimental Therapeutics, 304*(1), 162. doi:10.1124/jpet.102.043273

Kole, M. H. P., Hallermann, S., & Stuart, G. J. (2006). Single Ih Channels in Pyramidal Neuron Dendrites: Properties, Distribution, and Impact on Action Potential Output. *The Journal of Neuroscience, 26*(6), 1677. doi:10.1523/JNEUROSCI.3664-05.2006

Krnjević, K., Pumain, R., & Renaud, L. (1971). The mechanism of excitation by acetylcholine in the cerebral cortex. *The Journal of Physiology, 215*(1), 247-268.

Larsson, H. P. (2013). What determines the kinetics of the slow afterhyperpolarization (sAHP) in neurons? *Biophysical journal, 104*(2), 281-283. doi:10.1016/j.bpj.2012.11.3832

Lee, M. G., Hassani, O. K., Alonso, A., & Jones, B. E. (2005). Cholinergic Basal Forebrain Neurons Burst with Theta during Waking and Paradoxical Sleep. *The Journal of Neuroscience, 25*(17), 4365. doi:10.1523/JNEUROSCI.0178-05.2005

Libet, B., Gleason, C. A., Wright, E. W., & Pearl, D. K. (1983). Time of conscious intention to act in relation to onset of cerebral activity (readiness-potential). The unconscious initiation of a freely voluntary act. *Brain*.

Lindsley, D. B., Bowden, J. W., & Magoun, H. W. (1949). Effect upon the EEG of acute injury to the brain stem activating system. *Electroencephalography and Clinical Neurophysiology, 1*(1), 475-486. doi:https://doi.org/10.1016/0013-4694(49)90221-7

Lovinger, D. M. (2010). Neurotransmitter roles in synaptic modulation, plasticity and learning in the dorsal striatum. *Neuropharmacology, 58*(7), 951-961. doi:10.1016/j.neuropharm.2010.01.008

Lu, C. B., & Henderson, Z. (2010). Nicotine induction of theta frequency oscillations in rodent hippocampus in vitro. *Neuroscience, 166*(1), 84-93. doi:https://doi.org/10.1016/j.neuroscience.2009.11.072

Lüscher, C., & Malenka, R. C. (2012). NMDA receptor-dependent long-term potentiation and long-term depression (LTP/LTD). *Cold Spring Harbor perspectives in biology, 4*(6), a005710. doi:10.1101/cshperspect.a005710

Lörincz, A., Notomi, T., Tamás, G., Shigemoto, R., & Nusser, Z. (2002). Polarized and compartment-dependent distribution of HCN1 in pyramidal cell dendrites. *Nature Neuroscience, 5*(11), 1185-1193. doi:10.1038/nn962

Madison, D. V., & Nicoll, R. A. (1986). Actions of noradrenaline recorded intracellularly in rat hippocampal CA1 pyramidal neurones, in vitro. *The Journal of Physiology, 372*, 221-244.

Magee, J. C. (1999). Dendritic Ih normalizes temporal summation in hippocampal CA1 neurons. *Nature Neuroscience, 2*, 508. doi:10.1038/9158

Magee, J. C., & Johnston, D. (2005). Plasticity of dendritic function. *Current Opinion in Neurobiology, 15*(3), 334-342. doi:https://doi.org/10.1016/j.conb.2005.05.013

Markram, H., Lübke, J., Frotscher, M., & Sakmann, B. (1997). Regulation of Synaptic Efficacy by Coincidence of Postsynaptic APs and EPSPs. *Science, 275*(5297), 213. doi:10.1126/science.275.5297.213

Marrosu, F., Portas, C., Mascia, M. S., Casu, M. A., Fà, M., Giagheddu, M., . . . Gessa, G. L. (1995). Microdialysis measurement of cortical and hippocampal acetylcholine release during sleep-wake cycle in freely moving cats. *Brain Research, 671*(2), 329-332. doi:https://doi.org/10.1016/0006-8993(94)01399-3

Martella, G., De Persis, C., Bonsi, P., Natoli, S., Cuomo, D., Bernardi, G., . . . Pisani, A. (2005). Inhibition of Persistent Sodium Current Fraction and Voltage-gated L-type Calcium Current by Propofol in Cortical Neurons: Implications for Its Antiepileptic Activity. *Epilepsia, 46*(5), 624-635. doi:10.1111/j.1528-1167.2005.34904.x

Matthews, E. A., Linardakis, J. M., & Disterhoft, J. F. (2009). The fast and slow afterhyperpolarizations are differentially modulated in hippocampal neurons by aging and learning. *The Journal of neuroscience : the official journal of the Society for Neuroscience, 29*(15), 4750-4755. doi:10.1523/JNEUROSCI.0384-09.2009

Maurer, F., Lorenz, D. J., Pielsticker, G., Volk, T., Sessler, D. I., Baumbach, J. I., & Kreuer, S. (2017). Adherence of volatile propofol to various types of plastic tubing. *Journal of Breath Research, 11*(1), 016009. doi:10.1088/1752-7163/aa567e

McCormick, D. A., & Prince, D. A. (1986). Mechanisms of action of acetylcholine in the guinea-pig cerebral cortex in vitro. *The Journal of Physiology, 375*, 169-194.

McNaughton, B. L., Douglas, R. M., & Goddard, G. V. (1978). Synaptic enhancement in fascia dentata: Cooperativity among coactive afferents. *Brain Research, 157*(2), 277-293. doi:https://doi.org/10.1016/0006-8993(78)90030-6

Medic, G., Wille, M., & Hemels, M. E. (2017). Short- and long-term health consequences of sleep disruption. *Nature and science of sleep, 9*, 151-161. doi:10.2147/NSS.S134864

Mesulam, M. M., Mufson, E. J., Levey, A. I., & Wainer, B. H. (1983). Cholinergic innervation of cortex by the basal forebrain: Cytochemistry and cortical connections of the septal area, diagonal band nuclei, nucleus basalis (Substantia innominata), and hypothalamus in the rhesus monkey. *Journal of Comparative Neurology, 214*(2), 170-197. doi:10.1002/cne.902140206

Mesulam, M. M., Mufson, E. J., Wainer, B. H., & Levey, A. I. (1983). Central cholinergic pathways in the rat: An overview based on an alternative nomenclature (Ch1–Ch6). *Neuroscience, 10*(4), 1185-1201. doi:https://doi.org/10.1016/0306-4522(83)90108-2

Minkel, J., Htaik, O., Banks, S., & Dinges, D. (2011). Emotional expressiveness in sleep-deprived healthy adults. *Behavioral sleep medicine, 9*(1), 5-14. doi:10.1080/15402002.2011.533987

Monaghan, D. T., Irvine, M. W., Costa, B. M., Fang, G., & Jane, D. E. (2012). Pharmacological modulation of NMDA receptor activity and the advent of negative and positive allosteric modulators. *Neurochemistry international, 61*(4), 581-592. doi:10.1016/j.neuint.2012.01.004

Moyer Jr, J. R., Thompson, L. T., & Disterhoft, J. F. (1996). Trace Eyeblink Conditioning Increases CA1 Excitability in a Transient and Learning-Specific Manner. *The Journal of Neuroscience, 16*(17), 5536. doi:10.1523/JNEUROSCI.16-17-05536.1996

Murasaki, O., Kaibara, M., Nagase, Y., Mitarai, S., Doi, Y., Sumikawa, K., & Taniyama, K. (2003). Site of Action of the General Anesthetic Propofol in Muscarinic M1 Receptor-Mediated Signal Transduction. *Journal of Pharmacology and Experimental Therapeutics, 307*(3), 995. doi:10.1124/jpet.103.055772

Nadim, F., & Bucher, D. (2014). Neuromodulation of neurons and synapses. *Current Opinion in Neurobiology, 29*, 48-56. doi:10.1016/j.conb.2014.05.003

Nagase, Y., Kaibara, M., Uezono, Y., Izumi, F., Sumikawa, K., & Taniyama, K. (1999). Propofol Inhibits Muscarinic Acetylcholine Receptor-Mediated Signal Transduction in <I>Xenopus</I> Oocytes Expressing the Rat M1 Receptor. *The Japanese Journal of Pharmacology, 79*(3), 319-325. doi:10.1254/jjp.79.319

Ngo-Anh, T. J., Bloodgood, B. L., Lin, M., Sabatini, B. L., Maylie, J., & Adelman, J. P. (2005). SK channels and NMDA receptors form a Ca2+-mediated feedback loop in dendritic spines. *Nature Neuroscience, 8*, 642. doi:10.1038/nn1449

Nitz, D., & Siegel, J. (1997). GABA release in the dorsal raphe nucleus: role in the control of REM sleep. *American Journal of Physiology-Regulatory, Integrative and Comparative Physiology, 273*(1), R451-R455. doi:10.1152/ajpregu.1997.273.1.R451

O'Keefe, J., & Dostrovsky, J. (1971). The hippocampus as a spatial map. Preliminary evidence from unit activity in the freely-moving rat. *Brain Research, 34*(1), 171-175. doi:https://doi.org/10.1016/0006-8993(71)90358-1

Ode, K. L., Katsumata, T., Tone, D., & Ueda, H. R. (2017). Fast and slow Ca2+-dependent hyperpolarization mechanisms connect membrane potential and sleep homeostasis. *Current Opinion in Neurobiology, 44*, 212-221. doi:https://doi.org/10.1016/j.conb.2017.05.007

Oh, M. M., Kuo, A. G., Wu, W. W., Sametsky, E. A., & Disterhoft, J. F. (2003). Watermaze Learning Enhances Excitability of CA1 Pyramidal Neurons. *Journal of Neurophysiology, 90*(4), 2171-2179. doi:10.1152/jn.01177.2002

Orser, B. A., Bertlik, M., Wang, L. Y., & MacDonald, J. F. (1995). Inhibition by propofol (2,6 di-isopropylphenol) of the N-methyl-D-aspartate subtype of glutamate receptor in cultured hippocampal neurones. *British Journal of Pharmacology, 116*(2), 1761-1768.

Pachitariu, M., Lyamzin, D. R., Sahani, M., & Lesica, N. A. (2015). State-dependent population coding in primary auditory cortex. *The Journal of neuroscience : the official journal of the Society for Neuroscience, 35*(5), 2058-2073. doi:10.1523/JNEUROSCI.3318-14.2015

Pape, H. C. (1996). Queer Current and Pacemaker: The Hyperpolarization-Activated Cation Current in Neurons. *Annual Review of Physiology, 58*(1), 299-327. doi:10.1146/annurev.ph.58.030196.001503

Pedarzani, P., Krause, M., Haug, T., Storm, J. F., & Stühmer, W. (1998). Modulation of the Ca2+-Activated K+ Current sI AHP by aPhosphatase-Kinase Balance Under Basal Conditions inRat CA1 Pyramidal Neurons. *Journal of Neurophysiology, 79*(6), 3252-3256. doi:10.1152/jn.1998.79.6.3252

Pedarzani, P., & Storm, J. F. (1993). Pka mediates the effects of monoamine transmitters on the K+ current underlying the slow spike frequency adaptation in hippocampal neurons. *Neuron, 11*(6), 1023-1035. doi:https://doi.org/10.1016/0896-6273(93)90216-E

Pedarzani, P., & Storm, J. F. (1995). Dopamine modulates the slow Ca(2+)-activated K+ current IAHP via cyclic AMP-dependent protein kinase in hippocampal neurons. *Journal of Neurophysiology, 74*(6), 2749-2753. doi:10.1152/jn.1995.74.6.2749

Petrovic, M. M., Nowacki, J., Olivo, V., Tsaneva-Atanasova, K., Randall, A. D., & Mellor, J. R. (2012). Inhibition of post-synaptic Kv7/KCNQ/M channels facilitates long-term potentiation in the hippocampus. *PloS one, 7*(2), e30402-e30402. doi:10.1371/journal.pone.0030402

Picciotto, Marina R., Higley, Michael J., & Mineur, Yann S. (2012). Acetylcholine as a Neuromodulator: Cholinergic Signaling Shapes Nervous System Function and Behavior. *Neuron, 76*(1), 116-129. doi:https://doi.org/10.1016/j.neuron.2012.08.036

Pittson, S., Himmel, A. M., & MacIver, M. B. (2004). Multiple synaptic and membrane sites of anesthetic action in the CA1 region of rat hippocampal slices. *BMC neuroscience, 5*, 52-52. doi:10.1186/1471-2202-5-52

Power, A. E. (2004). Slow-wave sleep, acetylcholine, and memory consolidation. *Proceedings of the National Academy of Sciences of the United States of America, 101*(7), 1795-1796. doi:10.1073/pnas.0400237101

Robinson, R. B., & Siegelbaum, S. A. (2003). Hyperpolarization-Activated Cation Currents: From Molecules to Physiological Function. *Annual Review of Physiology, 65*(1), 453-480. doi:10.1146/annurev.physiol.65.092101.142734

Sanchez-Vives, M. V., Mattia, M., Compte, A., Perez-Zabalza, M., Winograd, M., Descalzo, V. F., & Reig, R. (2010). Inhibitory Modulation of Cortical Up States. *Journal of Neurophysiology, 104*(3), 1314-1324. doi:10.1152/jn.00178.2010

Sanders, R. D., Tononi, G., Laureys, S., & Sleigh, J. W. (2012). Unresponsiveness ≠ unconsciousness. *Anesthesiology, 116*(4), 946-959. doi:10.1097/ALN.0b013e318249d0a7

Schwindt, P. C., Spain, W. J., Foehring, R. C., Chubb, M. C., & Crill, W. E. (1988). Slow conductances in neurons from cat sensorimotor cortex in vitro and their role in slow excitability changes. *Journal of Neurophysiology, 59*(2), 450-467. doi:10.1152/jn.1988.59.2.450

Scoville, W. B., & Milner, B. (1957). Loss of recent memory after bilateral hippocampal lesions. *Journal of neurology, neurosurgery, and psychiatry, 20*(1), 11-21.

Shi, S.-H., Hayashi, Y., Petralia, R. S., Zaman, S. H., Wenthold, R. J., Svoboda, K., & Malinow, R. (1999). Rapid Spine Delivery and Redistribution of AMPA Receptors After Synaptic NMDA Receptor Activation. *Science, 284*(5421), 1811. doi:10.1126/science.284.5421.1811

Soon, C. S., Brass, M., Heinze, H.-J., & Haynes, J.-D. (2008). Unconscious determinants of free decisions in the human brain. *Nature Neuroscience, 11*, 543. doi:10.1038/nn.2112

https://www.nature.com/articles/nn.2112#supplementary-information

Steriade, M. (2004). Acetylcholine systems and rhythmic activities during the waking–sleep cycle. In *Progress in brain research* (Vol. 145, pp. 179-196): Elsevier.

Thakkar, M. M. (2011). Histamine in the regulation of wakefulness. *Sleep medicine reviews, 15*(1), 65-74. doi:10.1016/j.smrv.2010.06.004

Thompson, L. T., Moyer, J. R., & Disterhoft, J. F. (1996). Transient changes in excitability of rabbit CA3 neurons with a time course appropriate to support memory consolidation. *Journal of Neurophysiology, 76*(3), 1836-1849. doi:10.1152/jn.1996.76.3.1836

Thompson, S. M., Masukawa, L. M., & Prince, D. A. (1985). Temperature dependence of intrinsic membrane properties and synaptic potentials in hippocampal CA1 neurons in vitro. *The Journal of Neuroscience, 5*(3), 817. doi:10.1523/JNEUROSCI.05-03-00817.1985

Tobler, I., & Borbély, A. A. (1986). Sleep EEG in the rat as a function of prior waking. *Electroencephalography and Clinical Neurophysiology, 64*(1), 74-76. doi:https://doi.org/10.1016/0013-4694(86)90044-1

Tombaugh, G. C., Rowe, W. B., & Rose, G. M. (2005). The Slow Afterhyperpolarization in Hippocampal CA1 Neurons Covaries with Spatial Learning Ability in Aged Fisher 344 Rats. *The Journal of Neuroscience, 25*(10), 2609. doi:10.1523/JNEUROSCI.5023-04.2005

Tzingounis, A. V., Kobayashi, M., Takamatsu, K., & Nicoll, R. A. (2007). Hippocalcin gates the calcium activation of the slow afterhyperpolarization in hippocampal pyramidal cells. *Neuron, 53*(4), 487-493. doi:10.1016/j.neuron.2007.01.011

Vyazovskiy, V. V., & Harris, K. D. (2013). Sleep and the single neuron: the role of global slow oscillations in individual cell rest. *Nature reviews. Neuroscience, 14*(6), 443-451. doi:10.1038/nrn3494

Vyazovskiy, V. V., Olcese, U., Hanlon, E. C., Nir, Y., Cirelli, C., & Tononi, G. (2011). Local sleep in awake rats. *Nature, 472*, 443. doi:10.1038/nature10009

https://www.nature.com/articles/nature10009#supplementary-information

Vyazovskiy, V. V., Olcese, U., Lazimy, Y. M., Faraguna, U., Esser, S. K., Williams, J. C., . . . Tononi, G. (2009). Cortical firing and sleep homeostasis. *Neuron, 63*(6), 865-878. doi:10.1016/j.neuron.2009.08.024

Walker, M. P., & Stickgold, R. (2004). Sleep-Dependent Learning and Memory Consolidation. *Neuron, 44*(1), 121-133. doi:https://doi.org/10.1016/j.neuron.2004.08.031

Wang, K., Mateos-Aparicio, P., Hönigsperger, C., Raghuram, V., Wu, W. W., Ridder, M. C., . . . Adelman, J. P. (2016). IK1 channels do not contribute to the slow afterhyperpolarization in pyramidal neurons. *eLife, 5*, e11206. doi:10.7554/eLife.11206

Whitt, J. P., Montgomery, J. R., & Meredith, A. L. (2016). BK channel inactivation gates daytime excitability in the circadian clock. *Nature Communications, 7*, 10837. doi:10.1038/ncomms10837

https://www.nature.com/articles/ncomms10837#supplementary-information
Wilson, C. (2008). Up and down states. *Scholarpedia journal*, *3*(6), 1410-1410.
Ying, S.-W., & Goldstein, P. A. (2005a). Propofol-Block of SK Channels in Reticular Thalamic Neurons Enhances GABAergic Inhibition in Relay Neurons. *Journal of Neurophysiology*, *93*(4), 1935-1948. doi:10.1152/jn.01058.2004
Ying, S.-W., & Goldstein, P. A. (2005b). Propofol suppresses synaptic responsiveness of somatosensory relay neurons to excitatory input by potentiating GABA(A) receptor chloride channels. *Molecular pain*, *1*, 2-2. doi:10.1186/1744-8069-1-2
Zoli, M., Torri, C., Ferrari, R., Jansson, A., Zini, I., Fuxe, K., & Agnati, L. F. (1998). The emergence of the volume transmission concept1Published on the World Wide Web on 12 January 1998.1. *Brain Research Reviews*, *26*(2), 136-147. doi:https://doi.org/10.1016/S0165-0173(97)00048-9

5 Appendix

5.1 Intrinsic properties

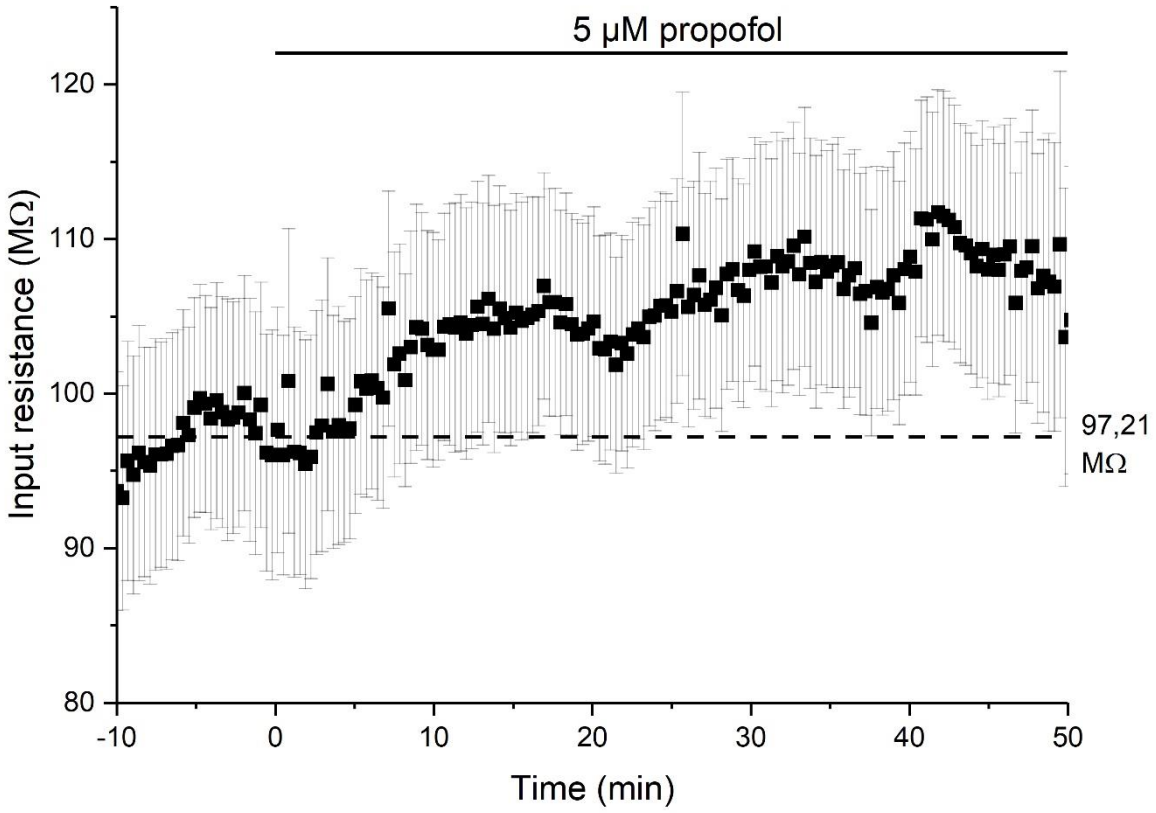

Figure 5.1: Average input resistance (n=18). Calculated as described in 2.5.1. Error bars represent SEM. The dotted line represents the average input resistance during baseline recording.

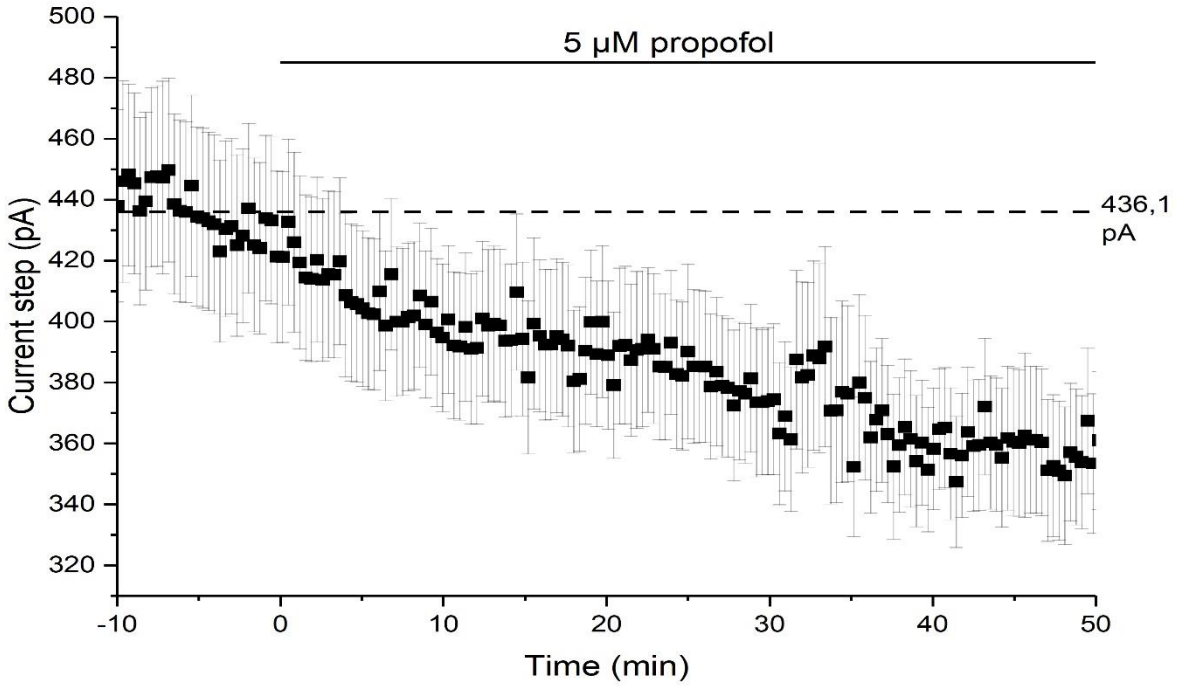

Figure 5.2: Average current size used to elicit 8 spikes in a 250 ms current step. All traces where more or fewer than 8 spike were elicited have been excluded. The dotted line represents the average current needed to elicit 8 spikes during baseline recordings.

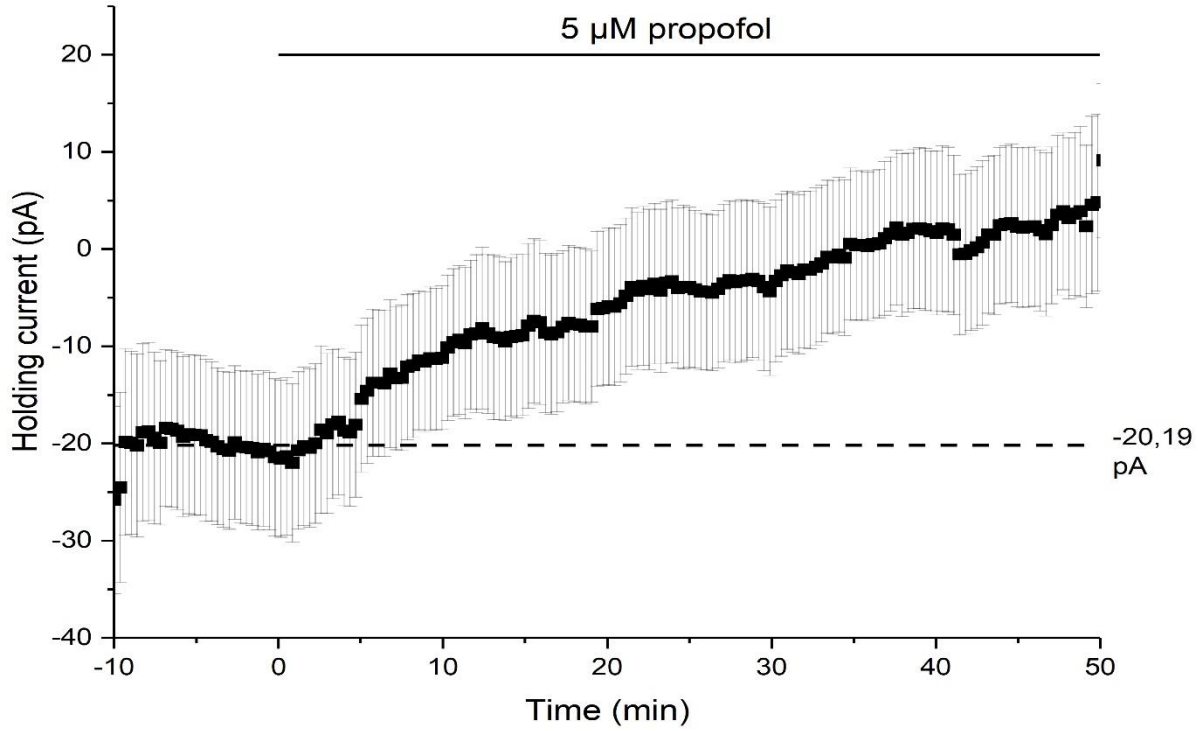

Figure 5.3: The average holding current used to hold the membrane potential at -65 mV. The dotted line represents the average holding current required to keep the RMP at -65 mV during baseline recordings

5.2 Solutions

5.2.1 Cutting solution

Table 5.1: 5x cutting stock solution.

	Molecular weight	**Concentration (mM)**	**Quantity (g/2L)**
NaCl	58.44	434.95	50.84
$NaHCO_3$	84.01	124.89	21.00
KCl	74.55	12.47	1.86
NaH_2PO_4	119.98	6.00	1.50

Table 5.2: Final cutting solution.

		Total concentration (mM)
	NaCl	87.00
	$NaHCO_2$	25.00
400 mL ddH_2O	KCl	2.50
100 mL cutting stock solution	NaH_2PO_4	1.25
128 g sucrose	Glucose	25.00
2.25 g glucose	Sucrose	74.80
0.5 mL 1M $CaCl_2$	$CaCl_2$	4.00
2 mL 1M $MgCl_2$	$MgCl_2$	1.00

5.2.2 Artificial cerebrospinal fluid (aCSF)

Table 5.3: 10x stock aCSF.

	Molecular weight	Concentration (mM)	Quantity (g/2L)
NaCl	58.44	1250.0	146.10
$NaHCO_3$	84.01	250.0	42.00
KCl	74.55	25.00	3.72
NaH_2PO_4	119.98	12.50	3.00

Table 6.4: Final aCSF solution.

		Total concentration (mM)
	NaCl	125.00
	$NaHCO_2$	25.00
900 mL ddH_2O	KCl	2.50
100 mL recording stock solution	NaH_2PO_4	1.25
2 g glucose	Glucose	10.00
1 mL 1M $CaCl_2$	$CaCl_2$	1.00
2 mL 1M $MgCl_2$	$MgCl_2$	2.00

5.2.3 Intracellular solution

Table 6.5: Intracellular pipette solution.

	[mM]	Molectular weight	g/100 mL
K-gluconate	120	234.25	2.8110
KCl	20	74.56	0.1491
NaATP	2	507.20	0.2029
$MgCl_2$	3	203.30	0.0600
HEPES	10	238.30	0.2383
NaGTP	0.4	623.20	0.0209